Pacific Northwest
NATIONAL LABORATORY

PNNL-30430 Rev. 1

Evaluation of Increased Peak Temperatures for Spent Fuel Cladding Performance during Dry Storage

September 2020

BE Wells,
NR Phillips
KJ Geelhood

Prepared for the U.S. Nuclear Regulatory Commission
Office of Nuclear Regulatory Research
Under Contract DE-AC05-76RL01830
Interagency Agreement: NRC-HQ-25-14-D-0001
Task Order Number: 31310018F0044

DISCLAIMER

PACIFIC NORTHWEST NATIONAL LABORATORY
operated by
BATTELLE
for the
UNITED STATES DEPARTMENT OF ENERGY
under Contract DE-AC05-76RL01830

Printed in the United States of America

Available to DOE and DOE contractors from the Office of Scientific and Technical Information,
P.O. Box 62, Oak Ridge, TN 37831-0062
www.osti.gov
ph: (865) 576-8401
fax: (865) 576-5728
email: reports@osti.gov

Available to the public from the National Technical Information Service
5301 Shawnee Rd., Alexandria, VA 22312
ph: (800) 553-NTIS (6847)
or (703) 605-6000
email: info@ntis.gov
Online ordering: http://www.ntis.gov

PNNL-30430 Rev. 1

Evaluation of Increased Peak Temperatures for Spent Fuel Cladding Performance during Dry Storage

September 2020

BE Wells,
NR Phillips
KJ Geelhood

Prepared for the U.S. Nuclear Regulatory Commission
Office of Nuclear Regulatory Research
Under Contract DE-AC05-76RL01830
Interagency Agreement: NRC-HQ-25-14-D-0001

Pacific Northwest National Laboratory
Richland, Washington 99354

Abstract

NUREG-2214, “Managing Aging Processes in Storage (MAPS) Report,” (2019) documents the technical basis for age-related degradation mechanisms on spent nuclear fuel assemblies during dry storage operations. The technical bases have been reviewed, and hoop cladding stress calculations were conducted using the Fuel Analysis under Steady-state and Transients (FAST) code at elevated normal condition temperatures of 425°C and 450°C, and at an off-normal and accident conditions temperature of 600°C. The NUREG-2214 conclusions are substantiated by the referenced literature. The calculations demonstrate that the aging mechanisms primarily driven by hoop stress such as hydride reorientation, delayed hydride cracking, thermal and athermal (low-temperature) creep, and localized mechanical overload are either not credible or do not compromise the fuel assembly’s performance for increased peak normal condition temperatures of 425°C or 450°C during the up to 60-year dry storage period. Other aging mechanisms considered are also not credible for compromising the fuel assembly’s performance during 60-year dry storage with a peak temperature of 400ºC as specified in ISG – 11 Rev. 3, and the same is indicated for the increased peak normal condition temperatures of 425°C or 450°C.

Acronyms and Abbreviations

BWR	boiling water reactor
DBTT	ductile-to-brittle transition temperature
DSS	dry storage system
EPRI	Electric Power Research Institute
FAST	Fuel Analysis under Steady-state and Transients
IFBA	integral fuel burnable absorber
ISG	Interim Staff Guidance
NRC	U.S. Nuclear Regulatory Commission
PNNL	Pacific Northwest National Laboratory
PWR	pressurized water reactor
SCC	stress corrosion cracking
SNF	spent nuclear fuel
UTS	ultimate tensile strength

Contents

Figures

Tables

1.0 Introduction

Pacific Northwest National Laboratory (PNNL) supports a wide range of technical and scientific disciplines, in accomplishing work-related activities aimed at ensuring the overall safety, security, and adequacy of nuclear power plant design, construction, operations, and environmental protection under U.S. Nuclear Regulatory Commission (NRC) Task Order 31310018F0044. As part of that work, the temperature tolerance for spent nuclear fuel assembly components of high burnup fuel has been evaluated for specific age-related degradation mechanisms in up to 60 years of spent fuel storage.

NUREG-2214, "Managing Aging Processes in Storage (MAPS) Report," (2019) documents the technical basis for peak temperature during dry storage for age-related degradation mechanisms on spent nuclear fuel assemblies. The spent nuclear fuel assembly components evaluated include the zirconium-based cladding and fuel assembly hardware that provide structural support to ensure that the spent fuel is maintained in a known geometric configuration. The aging mechanisms considered for high burnup zirconium-based cladding (i.e., average assembly burnups exceeding 45 GWd/MTU) include hydride reorientation, delayed hydride cracking, thermal and athermal (low-temperature) creep, and localized mechanical overload. These mechanisms are primarily driven by the cladding hoop stresses.[1] Other aging mechanisms considered for both low and high burnup zirconium-based cladding include radiation embrittlement, fatigue, oxidation, pitting corrosion, galvanic corrosion, and stress corrosion cracking (SCC). The age-related degradation mechanisms considered for the assembly hardware include creep, fatigue, hydriding, general corrosion, SCC, and radiation embrittlement.

PNNL was requested to:

- Perform and document calculations using the Fuel Analysis under Steady-state and Transients (FAST) code to predict the cladding stress level associated with the following temperatures: 425°C, 450°C (normal conditions), and 600°C (off-normal and accident conditions).
- Document the relative impact of the higher cladding stress level associated with the higher cladding temperature on each age-related degradation mechanism driven by hoop stress.
- Evaluate and document the technical bases of NUREG-2214 and any additional literature for information about the temperature and associated cladding hoop stress on each age-related degradation mechanism. If temperature-driven or stress-driven failure limits are identified as appropriate for a degradation mechanism, the basis for the limit shall be documented. In cases where the evaluation provides a technical basis to revise the guidance in NUREG-2214 to support a temperature tolerance, PNNL shall provide suggested edits to the text in NUREG-2214.

[1] As summarized in NUREG-2214, hoop stresses are lower in low burnup fuel. It was therefore noted that as the technical bases for the listed mechanisms primarily driven by hoop stress considered cladding hoop stresses for high burnup fuel, the discussions were considered bounding to low burnup fuel. Demonstration programs have provided confirmation that hydride reorientation and creep will not compromise the configuration of low burnup fuel during the renewal period (see NUREG-2214).

This report provides the documentation of the requested evaluations under the same assumption as in NUREG-2214 that the cladding is intact.[1] A brief background summary is provided in Section 2.0. Calculated hoop stresses as evaluated by the FAST code are presented in Section 4.0, and these results are evaluated with respect to the age-related degradation mechanisms in Section 5.0. A summary of the results is provided in Section 6.0.

[1] From Interim Staff Guidance – 1, Revision 2, “Intact SNF - Any fuel that can fulfill all fuel-specific and system-related functions, and that is not breached. Note that all intact SNF is undamaged, but not all undamaged fuel is intact, since under most situations, breached spent fuel rods that are not grossly breached will be considered undamaged.” SNF – spent nuclear fuel.

2.0 Background

After operation in a reactor, spent fuel assemblies are removed from the reactor and allowed to cool in storage pools that have continuously flowing water. Following sufficient cooling, the spent fuel assemblies are removed from wet storage and loaded into a dry storage system (DSS). The DSS confinement cavity (canister or cask) is vacuum dried at an increased temperature, backfilled with an inert gas, and welded/bolted shut. Example pressurized water reactor (PWR) and boiling water reactor (BWR) fuel assemblies are shown in Figure 2.1. In addition to the fuel rods, the assembly hardware analyzed in NUREG-2214 included the guide tubes, spacer grids, and lower and upper end fittings. An example image of a DSS cask is provided in Figure 2.2, with a fuel assembly canister enclosed.

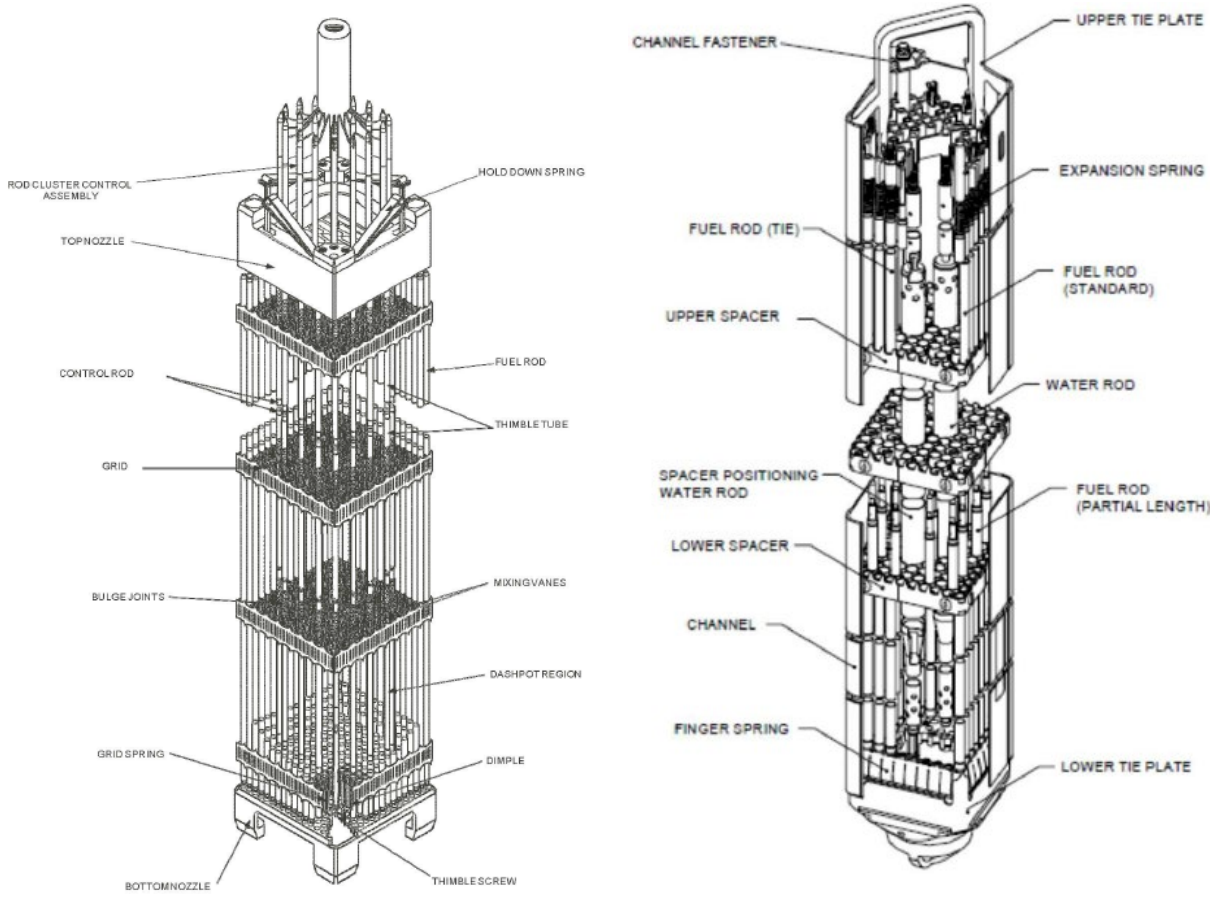

a) b)

Figure 2.1. Example Fuel Assemblies a) PWR, b) BWR (from NUREG-2214)

Figure 2.2. Example DSS Cask (from https://www.nrc.gov/reading-rm/doc-collections/infographics/dry-storage-of-spent-nuclear-fuel.png)

The generically allowable[1] maximum or peak temperature during the process is specified in Interim Staff Guidance – 11 (hereafter referred to as ISG – 11), Revision 3, "Cladding Considerations for the Transportation and Storage of Spent Fuel," as follows:

> "For all fuel burnups (low and high), the maximum calculated fuel cladding temperature should not exceed 400ºC (752ºF) for normal conditions of storage and short-term loading operations (e.g., drying, backfilling with inert gas, and transfer of the cask to the storage pad).
>
> However, for low burnup fuel, a higher short-term temperature limit may be used, if the applicant can show by calculation that the best estimate cladding hoop stress is equal to or less than 90 MPa (13,053 psi) for the temperature limit proposed."

Further,

> "The staff believes that this guidance will allow all commercial spent fuel that is currently licensed by the Nuclear Regulatory Commission (NRC) for commercial power plant operations to be stored in accordance with the regulations contained in 10 CFR Part 72."

The regulations for storage, as given in 10 CFR Part 72 have the following common safety objectives:

1) Ensure that the doses are less than the limits prescribed in the regulations, see 72.104 and 72.106.

[1] The guidance in ISG-11, Revision 3, defines a generic peak cladding temperature for zirconium-based alloys. Applicants are not expected to provide a technical basis in support of this generic limit. The NRC will review applications at higher peak cladding temperatures if an adequate technical basis is provided.

2) Maintain subcriticality under all credible conditions of storage (see 72.236(c)) and transportation (10 CFR Part 71, not addressed herein).

3) Ensure there is adequate confinement and containment of the spent fuel under all credible conditions of storage (see 72.236(e)) and transportation (10 CFR Part 71, not addressed herein).

More specifically, 10 CFR 72.122(h)(1),

> "The spent fuel cladding must be protected during storage against degradation that leads to gross ruptures or the fuel must be otherwise confined such that degradation of the fuel during storage will not pose operational safety problems with respect to its removal from storage."

10 CFR 72.122(l)

> "Retrievability. Storage systems must be designed to allow ready retrieval of spent fuel, high-level radioactive waste, and reactor-related GTCC waste for further processing or disposal."

and 10 CFR 72.124(a),

> "Spent fuel handling, packaging, transfer, and storage systems must be designed to be maintained subcritical and to ensure that, before a nuclear criticality accident is possible, at least two unlikely, independent, and concurrent or sequential changes have occurred in the conditions essential to nuclear criticality safety. The design of handling, packaging, transfer, and storage systems must include margins of safety for the nuclear criticality parameters that are commensurate with the uncertainties in the data and methods used in calculations and demonstrate safety for the handling, packaging, transfer and storage conditions and in the nature of the immediate environment under accident conditions."

These requirements form the basis of discussion via material degradation when describing the relative impact of the higher temperatures (i.e., above 400ºC).

3.0 Quality Assurance

This work was conducted with funding from the NRC under NRC Agreement No. NRC-HQ-25-14-D-0001, NRC Task Order 31310018F0044.

All research and development work at PNNL is performed in accordance with PNNL's Laboratory-level Quality Management Program, which is based on a graded application of NQA-1-2000, *Quality Assurance Requirements for Nuclear Facility Applications* (ASME 2000), to research and development activities. All staff members contributing to the work received appropriate technical and quality assurance training prior to performing quality-affecting work.

4.0 FAST Hoop Stress Calculations

Calculations were conducted to predict the cladding stress level associated with temperatures of 400°C (normal condition), 425°C and 450°C (elevated normal conditions), and 600°C (off-normal and accident conditions). FAST is a fuel thermal-mechanical code that has been developed and maintained by PNNL under contract for the NRC. The code is used to predict the component temperatures and deformations in a light water reactor fuel rod under steady-state and transient conditions.

FAST has been assessed against a large database of commercial and test reactor fuel rods and has been found to provide good predictions of parameters of interest, including rod internal pressure and void volume (Porter et al. 2020a). FAST, and its predecessor, FRAPCON (e.g., Geelhood et al. 2015), have been used to model spent fuel in the fuel pool as well as during various vacuum drying scenarios (Richmond and Geelhood 2018).

Calculations were conducted for BWR and PWR (including integral fuel burnable absorber [IFBA] fuel pellets) spent fuel. For the BWR fuel, a generalized 10 X 10 fuel design was used. For PWR fuel, two designs were studied: 17 X 17 design with UO_2 pellets and a 17 X 17 design with an IFBA coating. The rod average burnup was 45.17 GWd/MTU for the BWR case and 55.02 GWd/MTU and 57.30 GWd/MTU for the two PWR cases. As described in Richmond and Geelhood (2018), three different axial temperature profiles designated “vacuum,” “mid flow,” and “high flow” were generated based on thermal modeling experience and generalized models of storage systems for a range of conditions, Figure 4.1. The vacuum profile closely follows the heat generation profile of a spent fuel rod, indicating that there is no significant heat transfer due to convection, and is also characteristic of a horizontal module. In the mid flow case, the peak of the temperature profile sits in the top third of the active length of the fuel as is typical across a wide array of vertical storage systems. The high flow case represents analysis carried out on a system with particularly favorable convection conditions loaded at 100% design basis (i.e., maximum power allowed for maximum temperature of 400°C) and the temperature peak is near the plenum of the rod. Richmond and Geelhood (2018) note that it is unusual for the peak to be at this location during actual operation, but it is useful to investigate this case where the temperature peak is near the plenum of the rod because a high temperature in the plenum’s large free void volume will result in high rod internal pressure.

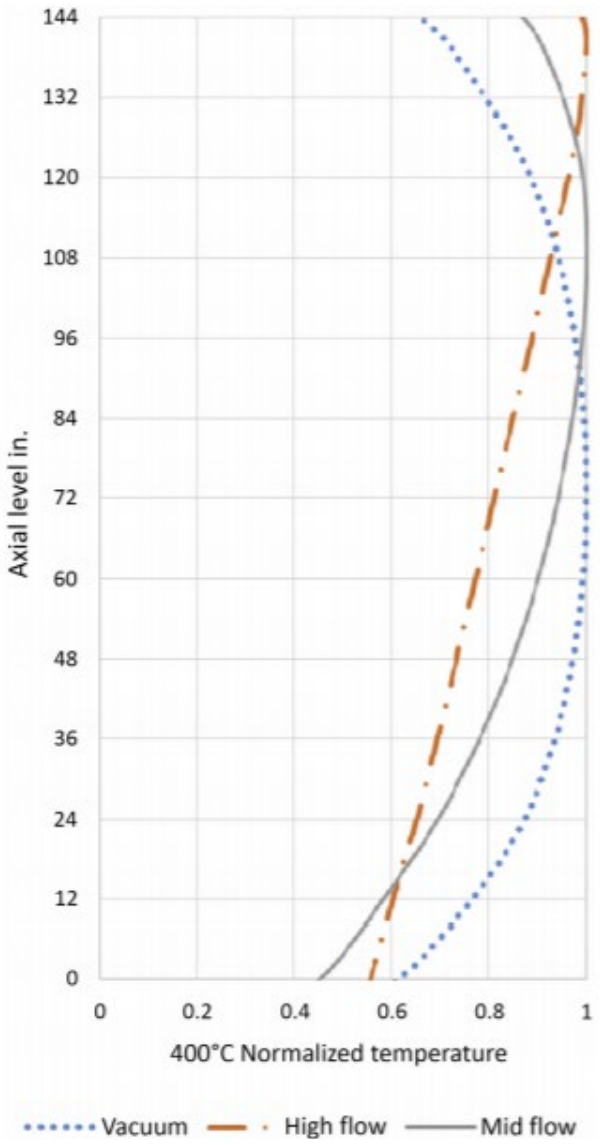

Figure 4.1. Normalized Temperature Profiles (Richmond and Geelhood 2018

Increased peak temperatures of 425°C and 450°C, representing the peak temperature during the vacuum drying process or initial cask loading, were evaluated for the resultant hoop stress with different cladding materials depending on the reactor type. The temperature profiles were created by adding 25°C and 50°C to the 400°C profiles of Richmond and Geelhood (2018). Bounding calculations were also conducted for the 600°C off-normal and accident conditions with a uniform axial profile for the cladding types with the highest calculated hoop stress at normal conditions (see discussion of results below). The uniform temperature profile is conservatively assumed, representing a blockage or fire condition, because a specific temperature profile is unknown and dependent on the specific scenario of interest. A summary of the FAST calculation cases is provided in Table 4.1.

Table 4.1. FAST Calculation Cases

Case	Axial Temperature Profile	Peak Fuel Rod Surface Temperatures (°C)	External Pressure (psia)(a)	Cladding Types(b)
Normal Conditions				
BWR	High flow Mid Flow Vacuum	400, 425, 450	90 14.7 0.06	Zircaloy-2
PWR	High flow			Zircaloy-4 ZIRLO™ Optimized ZIRLO™ M5®
PWR (IFBA)	High flow Mid Flow Vacuum		90 14.7 0.06	Zircaloy-4 ZIRLO™
Off-Normal and Accident Conditions				
BWR	Uniform	600	14.7	Zircaloy-2
PWR				Zircaloy-4 ZIRLO™
PWR (IFBA)				Zircaloy-4 ZIRLO™

(a) Although external pressures higher than 90 psia can exist, the 90 psia case was selected, as previously discussed, so that the temperature peak is near the plenum of the rod. Higher external pressures can counteract the rod internal pressure, thereby decreasing the hoop stress (e.g., see Richmond and Geelhood 2018).

(b) Zircaloy-2 Cold work = 0.0, Zircaloy-4 Cold work = 0.5, ZIRLO™ Cold work = 0.5, Optimized ZIRLO™ Cold work = 0.5, M5® Cold work = 0.0

Calculated cladding hoop stresses for normal conditions as functions of axial temperature profile, peak temperatures, external pressures, and cladding type are shown in Figure 4.2 through Figure 4.5. The 400°C results for all cases are in close agreement with those of Richmond and Geelhood (2018).[1] The results for the BWR fuel assemblies (Figure 4.2) also compare well under vacuum conditions with the 40 MPa maximum calculated hoop stress during drying operations at close to 400°C of Raynaud and Einziger (2015), although their burnup was substantially higher (~44% higher). For the PWR fuel assemblies, the Raynaud and Einziger (2015) maximum result of 100 MPa at 400°C is 100% larger than the maximum PWR and 2% larger than the maximum PWR (IFBA) results calculated herein, with the Raynaud and Einziger burnup approximately 18% higher.

In each figure for the primary variable of interest, the temperature increases of 25°C and 50°C result in approximately 4.5% and 9% increases, respectively, in the calculated hoop stress in comparison with the 400°C results. Consistent with Richmond and Geelhood (2018), the lowest calculated hoop stresses are achieved for the vacuum temperature profile, and the highest for the mid flow temperature profile. For the BWR case, the differences with temperature profile at each respective peak fuel rod surface temperature are on the order of 9% to 10%, and for the PWR (IFBA), approximately 4%. The calculated hoop stress results with the different claddings have a maximum difference of approximately 13% (PWR, Zircaloy-4 and M5® results).

[1] Slight differences in the results exist due to determination of a stress factor used to account for the fact that during reactor operations oxide buildup occurs and consumed some of the cladding metal.

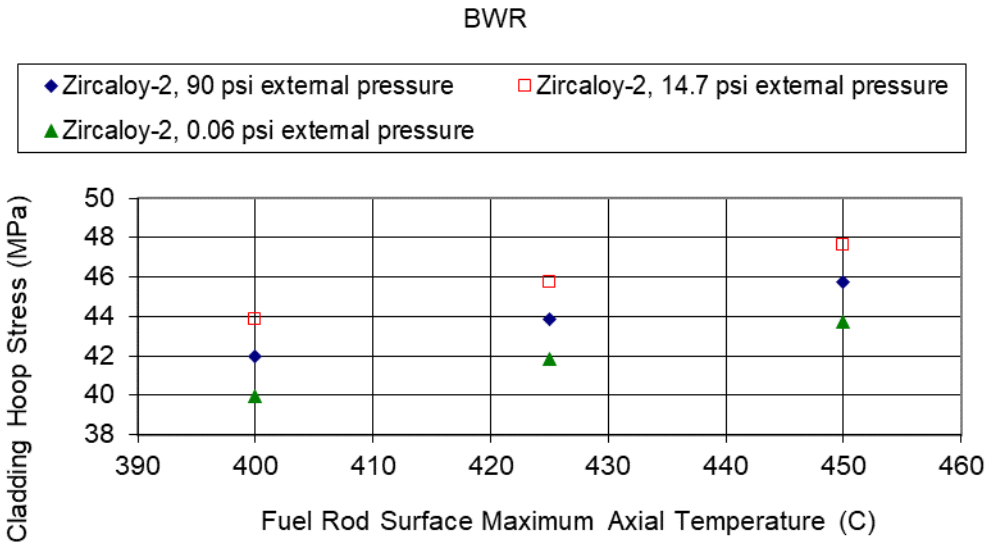

Figure 4.2. Calculated BWR Cladding Hoop Stress as a Function of Peak Fuel Rod Surface Temperature and External Pressure

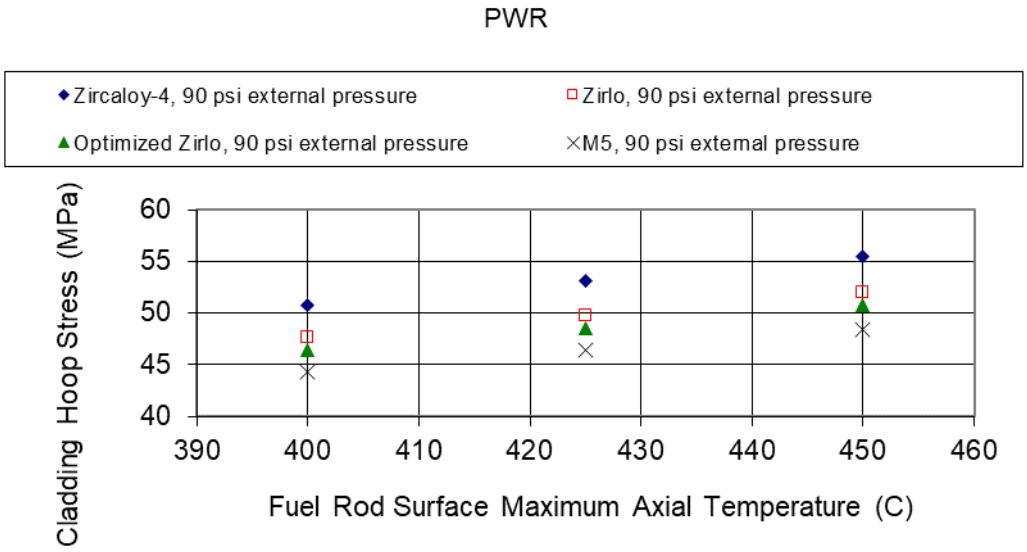

Figure 4.3. Calculated PWR Cladding Hoop Stress as a Function of Peak Fuel Rod Surface Temperature and Cladding Type

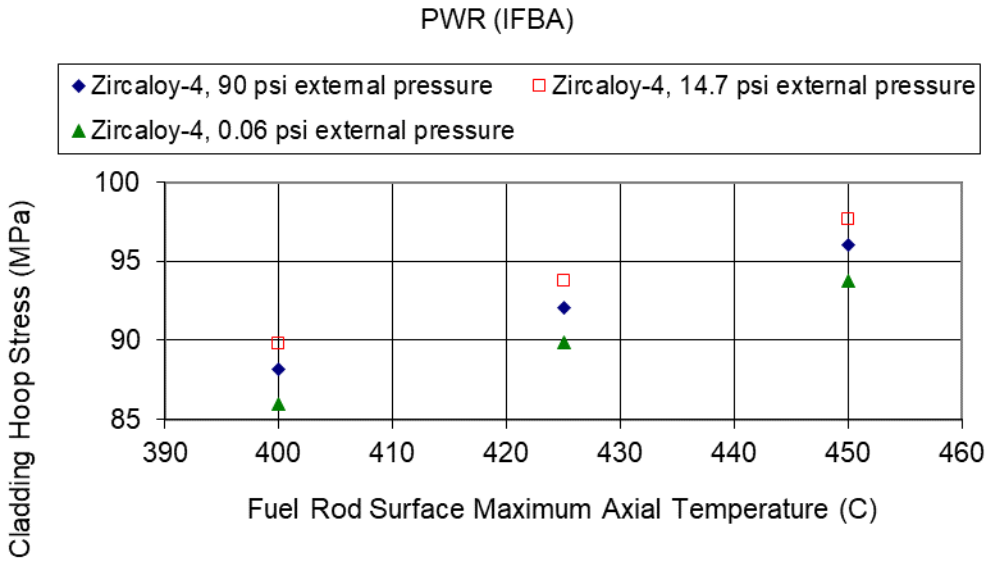

Figure 4.4. Calculated PWR (IFBA) Cladding Hoop Stress as a Function of Peak Fuel Rod Surface Temperature and External Pressure, Zircaloy-4 Cladding

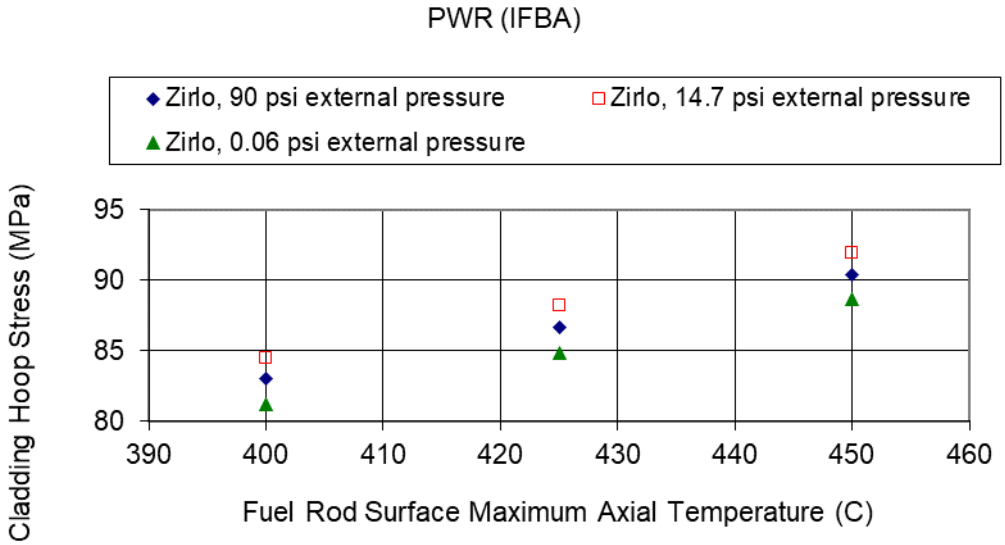

Figure 4.5. Calculated PWR (IFBA) Cladding Hoop Stress as a Function of Peak Fuel Rod Surface Temperature and External Pressure, ZIRLO™ Cladding

The calculated hoop stresses at the 600°C off-normal and accident conditions temperature with a uniform axial profile are shown in Figure 4.6. Increases ranging from approximately 27% to 65% over the corresponding minimum 400°C results are shown, with a maximum of approximately 133 MPa for the PWR (IFBA) fuel assembly with Zircaloy-4 cladding.

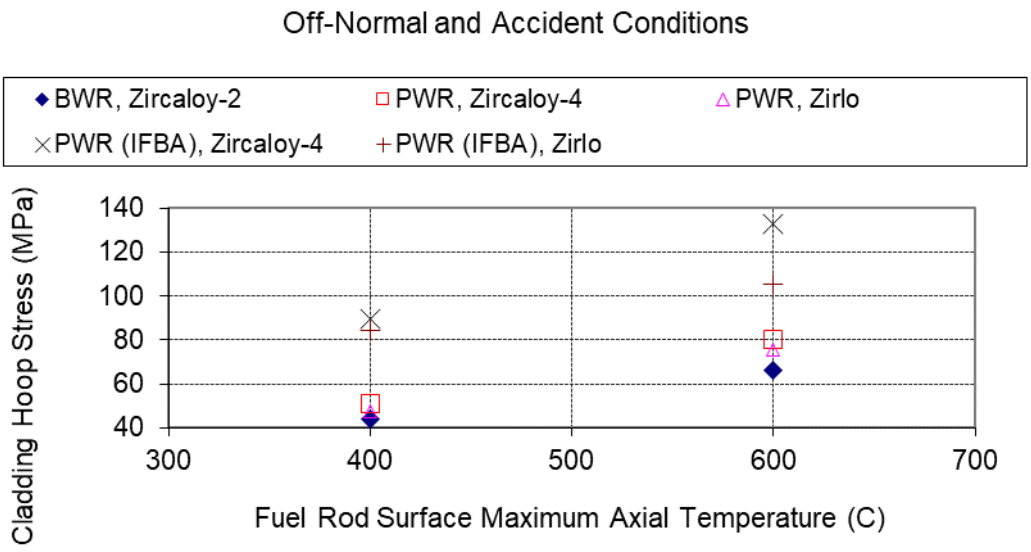

Figure 4.6. Calculated Cladding Hoop Stress at 600°C Representing an Off-normal and Accident Condition. 400°C results shown for comparison.

5.0 Peak Temperature Effects on Age-Related Degradation Mechanisms

The age-related degradation mechanisms primarily driven by the cladding hoop stresses for high burnup zirconium-based cladding include hydride reorientation, delayed hydride cracking, thermal and athermal (low-temperature) creep, and mechanical overload. The changes in the calculated cladding hoop stress due to the higher peak dry storage temperatures from Section 4.0 are discussed for each of these age-related degradation mechanisms.

Other aging mechanisms for zirconium-based cladding include radiation embrittlement, fatigue, oxidation, pitting corrosion, galvanic corrosion, and SCC. The age-related degradation mechanisms for the assembly hardware include creep, fatigue, hydriding, general corrosion, SCC, and radiation embrittlement.

5.1 Cladding Hoop Stress Driven Aging Mechanisms

The changes in the calculated cladding hoop stresses with higher peak temperatures (provided in Section 4.0) are discussed for the age-related degradation mechanisms primarily driven by the cladding hoop stresses for high burnup zirconium-based cladding.

5.1.1 Hydride Reorientation

Review of the technical bases presented in NUREG-2214 provided general concurrence with the conclusions presented therein for the effect of the maximum calculated fuel cladding temperature of 400ºC specified in ISG – 11 Rev. 3 on hydride reorientation. Radial hydride precipitation is credible in both BWR and PWR fuel claddings in dry storage, and the extent of hydride reorientation depends on cladding type and hydrogen content. However, the following statement in NUREG-2214:

> “review indicates that there is no consensus in the literature on threshold hoop stresses needed to reorient hydrides for a given cladding alloy and temperature”

is considered further with respect to whether (and the extent to which) hydride reorientation is indicated to occur for a specific cladding.

The threshold hoop stresses reported in NUREG-2214 for Zircaloy-4 at approximately 400°C range from nominally 60 to 120 MPa. The 60 MPa result is taken from Kim et al. (2015), which represents the onset temperature of the hydride reorientation from their test methodology, whereas the higher (more typically reported) temperatures for reorientation are the peak test

temperature.[1] The peak temperature of the 60 MPa hoop stress result for hydride reorientation is 461°C (Kim et al. 2015), in contrast to the reported onset temperature of 400°C. Kim et al. (2015) also note that it seems to be reasonable to correlate radial hydride reorientation with the peak temperature because the hydride reorientation did not occur without the high temperature preheating, and presented the data that way, as shown in Figure 5.1. Figure 5.1 also provides the Kim et al. (2015) data as well as other collected data from the literature on the hydride reorientation results in Zircaloy-4 (except the legend – denoted Bai [1994] RX sheet, Bai [1994] SR sheet, and Colas [2010] SR sheet) as a function of applied hoop stress and peak temperature, including data on non- and irradiated cladding. The Kim et al. (2015) results are shown to follow the lower bound of the other collected data, which is defined as the limit in which no reorientation occurs (note that the Kim et al. data are for a non-irradiated specimen). Comparison of this limit to the calculated hoop stresses presented in Section 4 is made following further discussion of these and other data.

The data shown in Figure 5.1 show a decreasing hoop stress for hydride reorientation with increasing temperature over approximately 275°C to 575°C of approximately −0.25 MPa/°C for the denoted lower hydride reorientation bound. Figure 5.1 includes data over 400°C collected from four different researchers. No significant change in the decreasing trend is indicated between 400°C and 450°C, and the data set of Kim et al. (2015), covering the largest peak temperature range (300°C to 461°C) of the data for any single investigation provided, may suggest a reduced MPa/°C with increasing temperature. A different trend in behavior below 400°C can potentially be suggested by the three data points of the legend-denoted Kamimura (2004) 48 GWd/tU data, with an increasing hoop stress with temperature from 300°C to 350°C. However, these limited data are suspect given the evidence of the other studies. Qualitatively similar behavior to the Kim et al. (2015) lower bound for Zircaloy-4 at temperatures from 350°C up to 470°C was presented in IAEA (2016), Figure 5.2.[2]

For unirradiated cladding samples, EPRI 2010 summarized that the precipitation of radial hydrides behavior in Zircaloy-4 and ZIRLO™ were similar. Machiels (2020) also grouped Zircaloy-4 and ZIRLO™ temperature – hoop stress – hydride reorientation behaviors together in a representatively linear fashion (decreasing hoop stress for hydride reorientation with increasing temperature) for 300°C to >400°C. In contrast, Machiels (2020) notes that recrystallized Zircaloy-2 cladding with a zirconium liner maintains its ductility in spite of hydride reorientation (see also Kamimura 2010). Inference of a change in hoop stress for hydride reorientation with increasing temperature for Zircaloy-2 from Kamimura (2010), which yields approximately −0.48 MPa/°C at both 50 and 55 GWd/MTU burnup, results in almost a factor of

[1] Kim et al. (2015) noted that the typical test method has a limitation in determining the threshold stress and temperature simultaneously because identification is made whether the reorientation occurs or not without specific identification of the onset temperature of the reorientation. They therefore modified their experimental procedures by adjusting the loading duration, which enabled to examination of both the threshold stress and the temperature. A ring tension method was used to apply a hoop stress to the cladding tube, and a finite element modeling analysis was accompanied to evaluate the stress distribution over the cladding thickness. A summary of hydride reorientation test methods is provided in IAEA (2015), and a number of mechanical test methods may be used to study the influence of radial hydrides on cladding embrittlement. Depending on the investigation, a ring compression test, uniaxial (hoop) ring stretch test, expansion due to compression test; or pressurized tube test may be utilized. IAEA (2015) also discusses that an issue in comparing testing results from various researchers is that a variety of measures of the hydride reorientation are typically used, and IAEA (2015) describes some of the quantification methods currently in use. Kim et al. (2015) do not qualify any of their conclusions related to Figure 5.1 due to any methodology differences that may be present in those data.

[2] The test conditions of the data presented in Figure 5.2 are indeterminate.

two increase above that of the lower bound line of Kim et al.(2015) shown in Figure 5.1 (−0.48 MPa/°C compared to the Kim et al. (2015) lower bound slope of −0.25 MPa/°C). This result is not unexpected given the noted hydride behaviors and relative hydrogen contents. Based on the available test data above 400°C and the relationships indicated by the data below that temperature, there is no indication identified of substantial behavioral change for the hoop stress for hydride reorientation with increasing peak temperature.

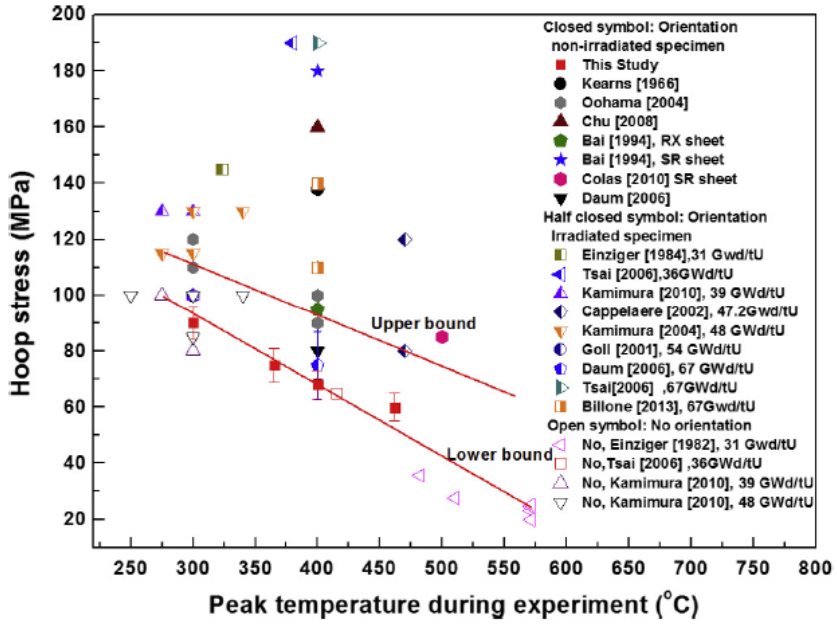

Figure 5.1. Hydride Reorientation in Zircaloy-4 as a Function of Peak Temperature and Cladding Hoop Stress (from Kim et al. 2015; citations for legend references provided therein)

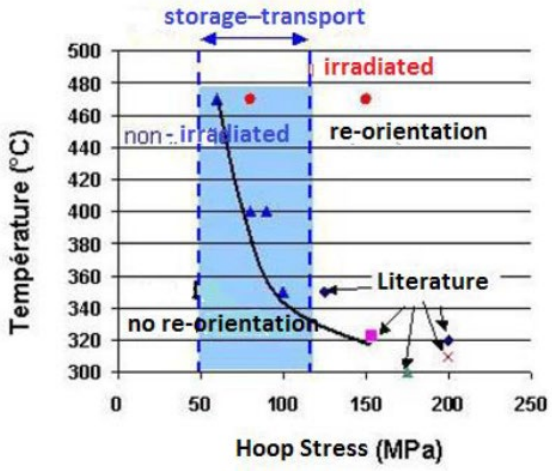

Figure 5.2. Hydride Reorientation as a Function of Temperature and Cladding Hoop Stress (from IAEA 2016, AREVA TN sponsored investigations)

For the NUREG-2214 reported maximum calculated hoop stress at 400°C of 100 MPa, hydride reorientation is indicated by Figure 5.1 by the ordinate, regardless of which temperature, the

peak temperature (461°C) or onset temperature (400°C), is considered. In contrast, the PWR fuel assembly with Zircaloy-4 cladding (non-IFBA) calculated hoop stress results from 400°C to 450°C (see Section 4.0), approximately 51 to 55 MPa, respectively, are below or just at the lower hydride reorientation limit, suggesting that hydride reorientation would not occur from the peak temperature increase. This illustration provides an example of the potential challenges of determining, from the previously quoted NUREG-2214 caution, "consensus in the literature … to reorient hydrides for a given cladding alloy and temperature."

For Zircaloy-4 cladding (IFBA), the calculated hoop stress results from 400°C to 450°C (see Section 4.0), approximately 86 to 98 MPa, are above the lower hydride reorientation limit of Kim et al. (2015), suggesting that hydride reorientation would be present throughout the evaluated temperature range. Given the previously noted differences in cladding behavior for temperature – hoop stress – hydride reorientation of Zircaloy-4 and Zircaloy-2, no comparison is made between the Kim et al. (2015) lower limit and FAST results for non- Zircaloy-4 claddings at elevated temperatures.

Regardless, based on the conclusion of NUREG-2214 that radial hydride precipitation is credible in both BWR and PWR fuel claddings in 60-year dry storage, given that the calculated cladding hoop stresses are shown to increase approximately 4.5% (at 425°C) and 9% (at 450°C) from the 400°C results (see Section 4.0), hydride reorientation is necessarily credible at higher temperatures. The extent of hydride reorientation to the radial direction becomes larger as the applied hoop stress increases above the critical stress at any given temperature (e.g., Machiels 2020). Further, the degradation of the mechanical properties at a particular temperature (described as the "ductile-to-brittle transition temperature" or DBTT, e.g., Billone et al. 2013) depends on the interconnectivity and number density of radial hydrides (NUREG-2214). Thus, the increased drying temperatures, with resultant, albeit slightly, increased hoop stress, may result in increased degradation of mechanical properties (i.e., lower ductility under hoop stress).

There are arguments against the significance of the potential minor increase in radial hydrides from peak temperature increases to 425°C or 450°C with respect to degradation of mechanical properties and cladding failure during dry storage. First, the acknowledged uncertainty in the data set did not preclude the conclusion in NUREG-2214 that "hydride reorientation is not expected to result in cladding failures and reconfiguration of the fuel, if the approved design bases are consistent with the acceptance criteria in ISG-11, Revision 3." The changes in calculated hoop stress due to the increased peak temperature are very small relative to the range of results and effect of competing and complimentary parameters (e.g., see Machiels 2020) in the data set at a given temperature, as exemplified by Figure 5.1. Thus, unless the NUREG-2214 conclusion was very close to a failure limit (which is not indicated by the available data), the NUREG-2214 conclusion is likely just as valid for the elevated peak temperatures of 425°C or 450°C.

Second, as noted in EPRI (2010) and Kamimura (2010), hydride reorientation does not necessarily correlate with embrittlement depending on the cladding material. Machiels (2020) concluded that when the alloy matrix strength (or yield stress) is less than the hydride fracture stress (~710 MPa), the presence of radial hydrides is largely irrelevant, except possibly in influencing the location at which ductile fracture eventually occurs. It is not clear from the presented data the extent to which this applies to all claddings and hydride concentrations and geometric distribution. However, a summary of cladding material mechanical properties is provided in Appendix A, and similar conclusions can be reached, strictly based on the hydride

fracture stress limit, with respect to different cladding types as described in Machiels (2020); the presence of radial hydrides is largely irrelevant.

5.1.2 Delayed Hydride Cracking

The literature discussed in NUREG-2214 provides the technical bases that delayed hydride cracking of the cladding is not credible during dry storage. Three conditions were listed as requisites for delayed hydride cracking: 1) hydrides, 2) existing crack tips, and 3) sufficient cladding hoop stresses. Given that the calculated hoop stress values (Section 4.0) at elevated peak temperatures of 425°C and 450°C are less than the bounding peak hoop stress values included in the NUREG-2214 evaluation, the evaluated peak temperatures above the ISG - 11, Rev. 3 limit of 400°C are not indicated to cause cladding failure during 60-year dry storage as a result of delayed hydride cracking.

5.1.3 Thermal Creep

The technical bases for thermal creep presented in NUREG-2214 demonstrate that cladding can be expected to undergo creep during dry storage. Thermal creep in a fuel rod under dry storage conditions is a self-limiting process and is strongly driven by both temperature and hoop stress.

For a spent fuel rod, the hoop stress is driven by gas pressure. Over time, the cladding temperature reduces as the heat load in the fuel rod decreases due to the decay of radionuclides in the spent fuel. This reduction in temperature leads to a corresponding reduction in creep rate. However, the actual creep of the cladding had the most pronounced impact on further creep rate because as the cladding strains, the void volume inside the rod is increased, thereby reducing the internal pressure and the hoop strain. Because fuel rods are so long, this void volume increase is significant. For example, in a spent fuel rod, 1% cladding strain will lead to a 30% increase in void volume. This increase in void volume corresponds to a similar drop in rod internal pressure and hoop strain. For this reason, thermal creep in a fuel rod under dry cask storage conditions is a self-limiting process, and additional creep will lead to a marked decrease in hoop stress, which is the driving force for further creep. A sample calculation starting at an initial hoop stress of 40 MPa was performed that shows for long-term creep, increasing the peak temperature at the beginning of cask loading will lead to more creep initially, but the long term creep rate for all these starting temperatures goes to a rate close to zero (See Figure 5.3).

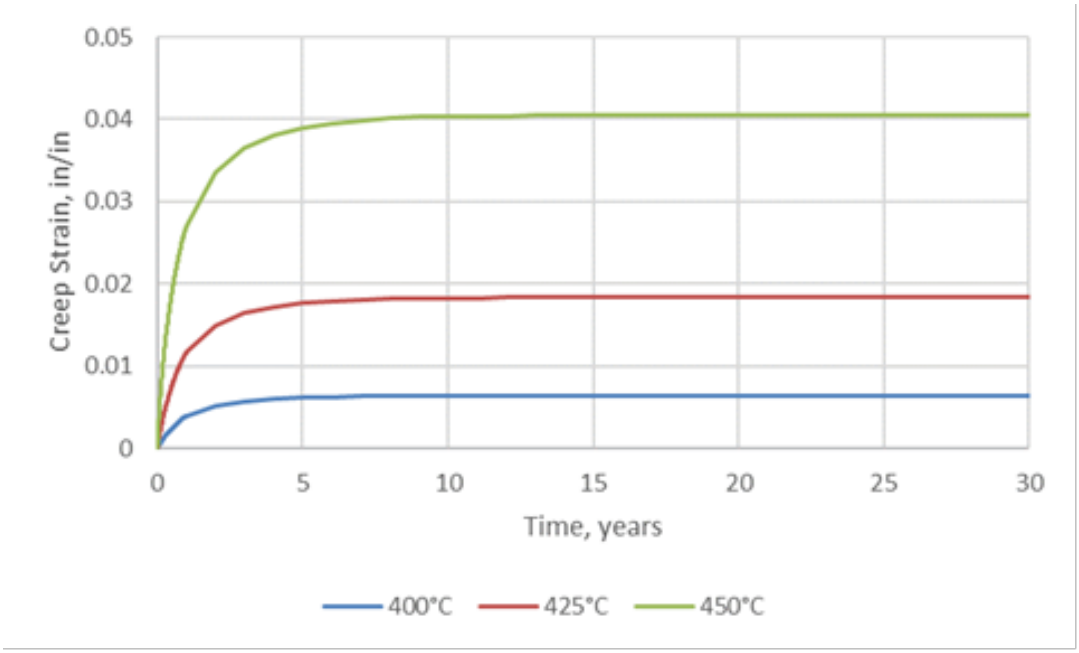

Figure 5.3. Sample creep strain calculation for spent fuel starting at a 40 MPa hoop stress for various peak cladding temperatures. A sample temperature decay curve was assumed for these cases.

The calculated cladding hoop stresses are shown in Section 4.0 to increase by approximately 4.5% (at 425°C) and 9% (at 450°C) from the 400°C results, with all normal and off-normal and accident condition calculated hoop stresses below the conditions analyzed for cladding hoop strain in NUREG-2214. Thus, based on the similar calculated final creep strains and limited increases in hoop stress, peak temperature increases to 425°C or 450°C from the ISG – 11, Rev. 3 limit of 400°C are not indicated to cause cladding failure during 60 year dry storage as a result of thermal creep.

5.1.4 Athermal Creep

The NUREG-2214 conclusion that the low-temperature (athermal) creep mechanism is not considered credible, even for the unlikely scenario where fuel reaches room temperature during dry storage, is substantiated by the technical bases presented therein. To bound this conclusion further, a non-physical comparison of the calculated hoop stress (Section 4.0) at elevated peak temperatures to the 25% of the yield strength criterion (NUREG-2214) for athermal creep for the room temperature cladding yield strength information (summarized in Appendix A) also indicates that the athermal creep mechanism is not credible.

5.1.5 Mechanical Overload

The technical bases presented in NUREG-2214 for mechanical overload were reviewed and confirm the conclusion that cladding failures due to pellet-cladding mechanical interaction-induced mechanical overload are not considered credible during dry storage at a peak temperature of 400ºC as specified in ISG – 11 Rev. 3. The NUREG-2214 basis discusses the creep strains previously determined relative to thermal creep and the associated hoop stresses. As for thermal creep, based on the similar calculated final creep strains and limited increases in hoop stress, peak temperature increases to 425°C or 450°C from the ISG – 11, Rev. 3 limit of

400°C are not indicated to cause cladding failure during 60-year dry storage as a result of mechanical overload.

5.2 Other Aging Mechanisms

The effects of higher peak temperatures during normal operations (i.e., 425°C or 450°C) on the other aging mechanisms evaluated in NUREG-2214 are discussed. These age-related degradation mechanisms apply to both low and high burnup zirconium-based cladding, and include oxidation, pitting corrosion, galvanic corrosion, SCC, radiation embrittlement, and fatigue. The age-related degradation mechanisms for the assembly hardware include creep, hydriding, general corrosion, SCC, radiation embrittlement, and fatigue.

5.2.1 Cladding

Oxidation

The conclusion given in NUREG-2214 is that oxidation is insignificant and aging management is not required during the 60-year timeframe. The basis for this conclusion is that there is not a significant quantity of water available for oxidation during dry storage. It was assumed that 1 L of water is significantly more than will be available after vacuum drying (0.43 moles per NUREG-2215), and even if this quantity of water were to completely react with the cladding, this would only represent less than 2% reduction in cladding thickness.

For an increase in peak temperature to 425°C or 450°C, the reaction rate of Zr with water is increased by a factor of 1.5 and 2.8 relative to 400°C (Jung et al. 2013). However, the argument from NUREG-2214 that the oxidation is source limited (limited water supply) still applies to the high temperature case. Therefore, it can be concluded that oxidation is insignificant and aging management is not required during the 60-year timeframe at a peak temperature of 425°C or 450°C.

Pitting Corrosion

The conclusion given in NUREG-2214 is that pitting corrosion of the cladding is not considered credible and aging management is not required during the 60-year timeframe. The basis for this conclusion is that there is not a significant quantity of water available to support the two requirements for pitting corrosion, namely that (1) there is an aggressive chemical environment that results in corrosion potential being greater than the repassivation potential and (2) there is enough cathodic capacity to sustain the propagation of the pitting corrosion (Shukla et al. 2008).

For an increase in peak temperature to 425°C or 450°C, the quantity of water is unchanged, or lower if vacuum drying was more effective at high temperature and is still not expected to be sufficient to provide enough cathodic capacity to initiate and propagate pitting corrosion of the cladding. Additionally, there are no mechanisms expected to be activated at 425°C or 450°C that would increase the aggressive chemical environment the cladding is exposed to. The outer surface of the cladding has no source of halides and, while iodine is present in the fuel as a fission product, none is expected to be released from the fuel at 400°C, 425°C, or 450°C according to the fission product release model in FAST (Porter et al 2020b). Additionally, there is little to no moisture inside a spent fuel rod.

Therefore, it can be concluded that pitting corrosion is not credible and aging management is not required during the 60 year timeframe at a peak temperature of 425°C or 450°C.

Galvanic Corrosion

The conclusion given in NUREG-2214 is that galvanic corrosion of the cladding is not considered credible and aging management is not required. The basis for this conclusion is that there is not a significant quantity of water available to support galvanic corrosion. For an increase in peak temperature to 425°C or 450°C the quantity of water is unchanged, or lower if vacuum drying was more effective at high temperature, and is still not expected to be sufficient to allow galvanic corrosion. Therefore, it can be concluded that pitting corrosion is not credible and aging management is not required at a peak temperature of 425°C or 450°C.

Stress Corrosion Cracking

The conclusion provided in NUREG-2214 is that SCC is not considered credible, and aging management is not required during the 60-year timeframe. The basis for this conclusion is drawn from a comparison of calculated/estimated maximum hoop stresses to a limit for the tensile stress indicated to be required for gross rupture (in the form of axial splitting induced by SCC). The tensile stress limit of 240 MPa for SCC used in NUREG-2214 is based on EPRI (1997) data for irradiated Zircaloy-2 and Zircaloy-4 over a temperature range of approximately 325°C to 360°C. Thus, the normal condition peak temperature of 400ºC specified in ISG – 11 Rev. 3 requires extrapolation from the data set employed for the NUREG-2214 conclusions.

Comparison of the calculated cladding hoop stresses presented in Section 4.0 at the elevated normal condition temperatures of 425°C and 450°C requires further extrapolation from the EPRI (1997) data set. The 4.5% (at 425°C) and 9% (at 450°C) increases in the cladding hoop stresses from the 400°C results do not threaten the 240 MPa criterion for SCC, and there is no basis within that data to indicate a change in behavior may be expected at higher temperatures. No data have been identified with SCC for temperatures above 360°C. However, the failure mechanism tests on irradiated Zircaloy-4 of Einziger et al. (1982) were conducted at temperatures of 482°C, 510°C, and 571°C and, while noted to be conducted at conditions where SCC would not be expected to be the cause of a breach, were also noted to have had no SCC with initial stresses of 39.8 to 75.7 MPa. As these stresses are on the order of and higher than the hoop stresses calculated in Section 4.0 for the non-IFBA fuel assemblies, it can be concluded from the available data for those assemblies that SCC is not credible and aging management is not required at a peak temperature of 425°C or 450°C.

Radiation Embrittlement

Radiation embrittlement is caused by fast neutron irradiation that creates defects in the metal crystal structure. These defects lead to a hardening of the bulk material that leads to an increase in strength and a decrease in ductility. Large enough neutron fluence can lead to a complete loss of ductility in the metal. Radiation hardening can be mitigated at increased temperature due to the annealing of these defects in the crystal structure. Most radiation hardening occurs in-reactor and concurrently with the production of defects the elevated cladding temperature serves to anneal some of these defects. The in-reactor annealing rate is less than the in-reactor production rate from neutron flux, so the cladding is hardened as it is irradiated.

When cladding is removed from the reactor, the neutron flux is essentially eliminated, although there is some small neutron flux in spent fuel from spontaneous fission events. In the case of storage at a peak temperature of 425°C or 450°C, it is expected that there will be slightly more annealing of radiation defects, which would lead to less hardening and actually result in

radiation embrittlement being less likely in these cases relative to a peak temperature of 400°C. Therefore, it can be concluded that radiation embrittlement is not credible and aging management is not required at a peak temperature of 425°C or 450°C.

Fatigue

The conclusion given in NUREG-2214 is that fatigue of the cladding is not considered credible, and aging management is not required. Calculations that assumed daily temperature fluctuations of 25°C and annual temperature fluctuations of 143°C for 60 years formed the basis for this conclusion. These calculations indicated that expected cumulative fatigue damage was between 20 and 115 MPa and was considerably lower than the fatigue failure threshold of 260 MPa.

For an increase in peak temperature to 425°C or 450°C there will be an increase in the gas pressure in the rods, but the change in pressure from the temperature variations will be the same as for the previous evaluation because this is driven by the ideal gas law. It is the change in pressure in this case, rather than the absolute pressure, that drives the fatigue loading. In this case, the previous analysis will also apply to the case of increased peak temperature.

As to the question of the effect of temperature on the cumulative fatigue failure criteria, although there is some amount of scatter in fatigue strength data, all the data sets that performed measurements on Zircaloy samples at various temperatures demonstrated some reduction in fatigue strength with increasing temperature. O'Donnell and Langer (1964) showed a small reduction in fatigue strength from 70°F to 600°F for unirradiated samples. Mehan and Wiesinger (1961) showed reduction in fatigue strength from 77°F to 600°F to 900°F for unirradiated samples. Pandarinathan and Vasudevan (1980) showed reduction in fatigue strength from 77°F to 572°F to 662°F. The typical irradiated fatigue design curve that is used is given by O'Donnell and Langer (1964) and has been found to be sufficiently conservative to bound all the temperature variations in other data except for those tested by Mehan and Wiesinger (1961) at 900°F. Irradiated Zircaloy exhibits a rapid decrease in yield strength at temperatures approaching 900°F (482°). This decrease in yield strength will cause a greater fraction of any cyclic strain to be plastic strain, which will most likely lead to lower fatigue strength. Additionally, this reduction is on the order of 5% and will not significantly impact the large margin previously calculated to the failure limit. Based on this, it is reasonable to retain the O'Donnell and Langer (1964) irradiated fatigue design curve as a failure criteria up to 450°C, but it should not be used for higher temperatures.

Therefore, it can be concluded that fatigue of the cladding is not credible and aging management is not required at a peak temperature of 425°C or 450°C.

5.2.2 Assembly Hardware

It is concluded in NUREG-2214 that none of the age-related degradation mechanisms(creep, hydriding, general corrosion, SCC, radiation embrittlement, or fatigue) considered for the assembly hardware (including the guide tubes, spacer grids, and lower and upper end fittings) require aging management for the 60-year storage period. These conclusions are supported by the referenced literature.

Creep

The conclusion given in NUREG-2214 is that creep of assembly components is not considered credible and aging management is not required. The basis for this conclusion is that by using a rule of thumb that the creep threshold is 40% of the melting temperature, it can be shown that the maximum temperature is below the creep threshold for each material. This basis is not particularly satisfying, since the expected creep threshold is below 400°C for Inconel and stainless steel. A better basis would be to cite that all subcomponents are not expected to experience sustained external loads during passive dry storage except from their own weight. Without significant loading, there is no potential for creep unless the weight of the assembly were applied to a thin component creating high stress. In a fuel assembly, all thin components (guide tubes and grid straps) are oriented such that the weight of the assembly is not applied to them. For an increase in peak temperature to 425°C or 450°C this situation remains the same.

Therefore, it can be concluded that creep of assembly components is not credible and aging management is not required at a peak temperature of 425°C or 450°C.

Hydriding

The conclusion given in NUREG-2214 is that hydriding of assembly components is not considered credible and aging management is not required. The basis for this conclusion is that hydriding is not an issue for steel and Inconel components and that for Zr components the loads are much lower than on fuel rods and hydride reorientation is not expected to occur. Also, any additional hydriding of the assembly hardware during extended storage is expected to be negligible (Jung et al. 2013). For an increase in peak temperature to 425°C or 450°C, the loads on Zr components will be unchanged and there is still not a significant quantity of hydrogen available for additional hydriding at these temperatures. Hydriding is not an issue for steel or Inconel components at these temperatures either.

Therefore, it can be concluded that hydriding of assembly components is not credible and aging management is not required at a peak temperature of 425°C or 450°C.

General Corrosion

The conclusion given in NUREG-2214 is that general corrosion of assembly components is not considered credible and aging management is not required. The basis for this conclusion is that there is not a significant quantity of water available for oxidation during dry storage. NUREG-2214 also cited very low corrosion rates for stainless steel and Inconel. For an increase in peak temperature to 425°C or 450°C, the quantity of water available is unchanged, or lower if vacuum drying was more effective at high temperature, and is still not expected to be sufficient to allow oxidation of assembly components even if the corrosion rates for stainless steel and Inconel are increased at elevated temperature.

Therefore, it can be concluded that general corrosion of assembly components is not credible and aging management is not required at a peak temperature of 425°C or 450°C.

Stress Corrosion Cracking

The conclusion given in NUREG-2214 is that SCC of assembly components is not considered credible and aging management is not required. The basis for this conclusion is that there is not a significant quantity of water available or halides for SCC oxidation during dry storage. For an

increase in peak temperature to 425°C or 450°C, the quantity of water available and lack of halides is unchanged or lower if vacuum drying was more effective at high temperature.

Therefore, it can be concluded that SCC corrosion of assembly components is not credible and aging management is not required at a peak temperature of 425°C or 450°C.

Radiation Embrittlement

The conclusion given in NUREG-2214 is that radiation embrittlement of assembly components is not considered credible and aging management is not required. The basis for this conclusion is that the neutron fluence is too low to cause significant increase in embrittlement for Zr, stainless steel, or Inconel. For an increase in peak temperature to 425°C or 450°C, the possibility of annealing radiation defects in all these materials increases and the potential for radiation embrittlement decreases relative to a peak temperature of 400°C.

Therefore, it can be concluded that radiation embrittlement of assembly components is not credible and aging management is not required at a peak temperature of 425°C or 450°C.

Fatigue

The conclusion given in NUREG-2214 is that fatigue of assembly components is not considered credible and aging management is not required. The basis for this conclusion is that these components are static components and loads on them will not be impacted by daily and annual temperature fluctuations. For an increase in peak temperature to 425°C or 450°C this situation remains the same.

Therefore, it can be concluded that fatigue of assembly components is not credible and aging management is not required at a peak temperature of 425°C or 450°C.

6.0 Summary

The technical bases for age-related degradation mechanisms on spent nuclear fuel assembly components of high burnup fuel documented in NUREG-2214, “Managing Aging Processes in Storage (MAPS) Report,” have been reviewed. The conclusions therein, that the aging mechanisms either are not credible or do not compromise the fuel assembly’s performance during 60-year dry storage with a peak temperature of 400ºC as specified in ISG – 11 Rev. 3, are substantiated by the referenced literature.

The same aging mechanisms were also reviewed in this report should the peak temperature be elevated to a normal condition temperature of 425°C or 450°C. The technical bases and data for the aging mechanisms, which are primarily driven by the cladding hoop stresses, were compared against calculated hoop stress results determined via the FAST code.

FAST hoop cladding stress calculations were conducted at the elevated normal condition temperatures. Calculations were also conducted at 600°C for off-normal and accident conditions. For the normal condition temperature increases for the specified representative fuel configurations and histories (modeled for three different temperature profiles representing a range of storage conditions), approximately 4.5% and 9% increases in hoop stress are respectively indicated over the 400°C result, regardless of the reactor or cladding type. A maximum cladding hoop stress of approximately 48 MPa is calculated for the BWR fuel assemblies at 450°C. For the PWR fuel assemblies, the maximum non-IFBA result is approximately 55 MPa at 450°C, and approximately 98 MPa for IFBA. For reference, the maximum calculated hoop stress for the 600°C for off-normal and accident conditions is approximately 133 MPa (PWR, IFBA). Based on these comparisons, the technical bases and reviewed data support that the aging mechanisms of hydride reorientation, delayed hydride cracking, thermal and athermal (low-temperature) creep, and localized mechanical overload either are not credible or do not compromise the fuel assembly’s performance for increased peak normal condition temperatures of 425°C and 450°C during the up to 60-year dry storage period.

Other aging mechanisms considered for both low and high burnup zirconium-based cladding include radiation embrittlement, fatigue, oxidation, pitting corrosion, galvanic corrosion, and SCC. The age-related degradation mechanisms considered for the assembly hardware include creep, fatigue, hydriding, general corrosion, SCC, and radiation embrittlement. For these mechanisms, the technical bases of NUREG-2214 demonstrate that the age-related degradation mechanisms are not credible for compromising the fuel assembly’s performance during 60-year dry storage with a peak temperature of 400ºC as specified in ISG – 11 Rev. 3, and the same is indicated for the increased peak normal condition temperatures of 425°C and 450°C.

7.0 References

10 CFR Part 71, “Packaging and Transportation of Radioactive Material.” *Code of Federal Regulations*.

10 CFR Part 72, “Licensing Requirements for the Independent Storage of Spent Nuclear Fuel, High-Level Radioactive Waste, and Reactor-Related Greater than Class C Waste.” *Code of Federal Regulations*.

ASME. 2000. *Quality Assurance Requirements for Nuclear Facility Applications*. NQA-1-2000, The American Society of Mechanical Engineers, New York, NY.

Billone MC, TA Burtseva, Z Han, and YY Liu. 2013. *Embrittlement and DBTT of High-Burnup PWR Fuel Cladding Alloys*. FCRD-UFD-2013-000401, ANL-13/16, Lemont, Illinois: Argonne National Laboratory. Einziger RE, SD Atkin, DE Stellrecht, and V Pasupathi. 1982. “High Temperature Postirradiation Materials Performance of Spent Pressurized Water Reactor Fuel Rods Under Dry Storage Conditions.” *Nuclear Technology* 57:65.

EPRI. 2010. *Hydride Reorientation Studies*. Product ID 1019097, Electric Power Research Institute. https://www.epri.com/research/products/1019097

EPRI. 1997. *Temperature Limit Determination of the Inert Dry Storage of Spent Nuclear Fuel*. Report TR-103949, Electric Power Research Institute, Palo Alto, CA.

Geelhood KJ, WG Luscher, PA Raynaud, and IE Porter. 2015. *FRAPCON-4.0: A Computer Code for the Calculation of Steady-State, Thermal-Mechanical Behavior of Oxide Fuel Rods for High Burnup*. PNNL-19418, Pacific Northwest National Laboratory, Richland, WA.

IAEA. 2016. *Cladding Embrittlement, Swelling, and Creep*. Workshop on Radiation Effects in Nuclear Waste Forms and Their Consequences for Storage and Disposal, September 12-16, 2016, Trieste, Italy.

IAEA. 2015. *Spent Fuel Performance*. *Final Report of a Coordinated Research Project on Spent Fuel Performance Assessment and Research (SPAR-III) 2009–2014*. IAEA-TECDOC-1771, International Atomic Energy Agency, Vienna, Austria.

Interim Staff Guidance 1, Revision 2. 2007. *Classifying the Condition of Spent Nuclear Fuel for Interim Storage and Transportation Based on Function*. ADAMS Accession No. ML063410468, U.S. Nuclear Regulatory Commission, Washington, D.C.

Interim Staff Guidance 11, Revision 3. 2003. *Cladding Considerations for the Transportation and Storage of Spent Fuel*. ADAMS Accession No. ML033230335, U.S. Nuclear Regulatory Commission, Washington, D.C.

Jung H, P Shukla, T Ahn, L Tipton, K Das, X He, and D Basu. 2013. *Extended Storage and Transportation: Evaluation of Drying Adequacy*. ADAMS Accession No. ML13169A039, San Antonio, Texas: Center for Nuclear Waste Regulatory Analyses. 2013.

Kamimura K. 2010. “Integrity Criteria for Spent Fuel Dry Storage in Japan.” *Proceeding of the International Seminar on Interim Storage of Spent Fuel, International Seminar on Spent Fuel Storage (ISSF)*. Tokyo, Japan. p. VI-3-1.

Kim JS, YJ Kim, DH Kook, and YS Kim. 2015. “A Study on Hydride Reorientation of Zircaloy4 Cladding Tube Under Stress.” *Journal of Nuclear Materials* 456:246–252.

Machiels A. 2020. *Effect of Hydride Reorientation in Spent Fuel Cladding—Status from Twenty Years of Research*. EPRI Technical Report 3002016033, J Kessler and Associates, LLC, Charlotte, NC.

Mehan RL and FW Wiesinger. 1961. Mechanical Properties of Zircaloy-2. KAPL-2110. AEC Research and Development Report, Knolls Atomic Power Laboratory, Schenectady, NY.

Miller L, D Basu, K Das, T Mintz, R Pabalan, G Walter, and G Oberson. 2013. *Overview of Vacuum Drying Methods and Factors Affecting the Quantity of Residual Water After Drying*. Center for Nuclear Waste Regulatory Analyses, San Antonio, TX.

NUREG-2214. 2019. *Managing Aging Processes in Storage (MAPS) Report*. U.S. Nuclear Regulatory Commission, Washington, D.C.

NUREG-2215. 2017. *Standard Review Plan for Spent Fuel Dry Storage Systems and Facilities*. U.S. Nuclear Regulatory Commission, Washington, D.C.

O’Donnell WJ, and BF Langer. 1964. Fatigue Design Basis for Zircaloy Components. *Nuclear Science and Engineering* 20:1-12 .

Pandarinathan PR, and P Vasudevan. 1980. Low-Cycle Fatigue Studies on Nuclear Reactor Zircaloy-2 Fuel Tubes at Room Temperature, 300, and 350°C. *Journal of Nuclear Materials*. 91(1980):47-58.

Porter IE, KJ Geelhood, D Richmond, DV Colameco, TZ Zipperer, EE Torres, WG Luscher, L Kyriazidis, and CE Goodson. 2020a. *FAST-1.0: Integral Assessment*. PNNL-29727, Pacific Northwest National Laboratory, Richland, WA.

Porter IE, KJ Geelhood, DV Colameco, EE Torres, WG Luscher, L Kyriazidis, and CE Goodson. 2020b. *FAST-1.0: A Computer Code for Thermal-Mechanical Nuclear Fuel Analysis under Steady-state and Transients*. PNNL-29720, Pacific Northwest National Laboratory, Richland, WA.

Raynaud PAC and RE Einziger. 2015. “Cladding Stress During Extended Storage of High Burnup Spent Nuclear Fuel.” *Journal of Nuclear Materials* 464:304–312.

Richmond DJ, and KJ Geelhood. 2018. “FRAPCON Analysis of Cladding Performance during Dry Storage Operations.” *Nuclear Engineering and Technology* 50(2):306-312.

Shukla PK, R Pabalan, T Ahn, L Yang, X He, and H Jung. 2013. “Cathodic Capacity of Alloy 22 in the Potential Yucca Mountain Repository Environment.” *Proceedings of the CORROSION 2008 Conference, Corrosion in Nuclear Systems Symposium.* New Orleans, LA, March 16–20, 2008. Paper No. 08583. Houston, TX: NACE International. 2008.

Appendix A – Tensile Strength as a Function of Temperature

This appendix provides a literature review on the tensile strength as a function of temperature for zirconium-based fuel cladding and fuel assembly hardware, specifically guide tubes, spacer grids, and lower and upper end fittings.

A.1 PWR and BWR Fuel Claddings

The following claddings presented below are Zircaloy-2, Zircaloy-4, ZIRLO™, and M5®. Optimized ZIRLO™ was omitted based on findings made by Beyer and Geelhood (2013), who noted that no mechanical property test data are available nor are there data on the hydride orientation of Optimized ZIRLO™ found in the open literature. Beyer and Geelhood (2013) also recommend that, in the absence of data, Westinghouse should be expected to use the M5® correlation for Optimized ZIRLO™ (pRXA); unless they can show data from irradiated Optimized ZIRLO™ that demonstrate that the hydrogen morphology in and uniform elongation of Optimized ZIRLO™ are the same as that of ZIRLO™.

Zircaloy-2 BWR Cladding

Geelhood et al. (2008) modeled predicted yield stress for pressurized water reactor (PWR; Zircaloy-4) and boiling water reactor (BWR; Zircaloy-2) conditions as a function of temperature, fast neutron fluence, cold work, and strain rate. Table A.1 shows the parameters of the model, Figure A.1 shows the results of the model. The predicted values for BWR at 700K (427°C) is ~500 MPa with a standard deviation of ±67 MPa.

Table A.1. Ranges of Fast Neutron Fluence, Cladding Type, Hydrogen Concentration, and Cold Work for PWR and BWR Cladding under Spent Fuel Conditions at 66 GWd/MTU (Geelhood et al. 2008)

	PWR	BWR
Fast neutron fluence	1.2×10^{26} n/m² (max)	1.2×10^{26} n/m² (max)
Cladding type	Zircaloy-4	Zircaloy-2
Cladding cold work	50%	0%
Hydrogen concentration	500 ppm (avg.)	250 ppm (avg.)

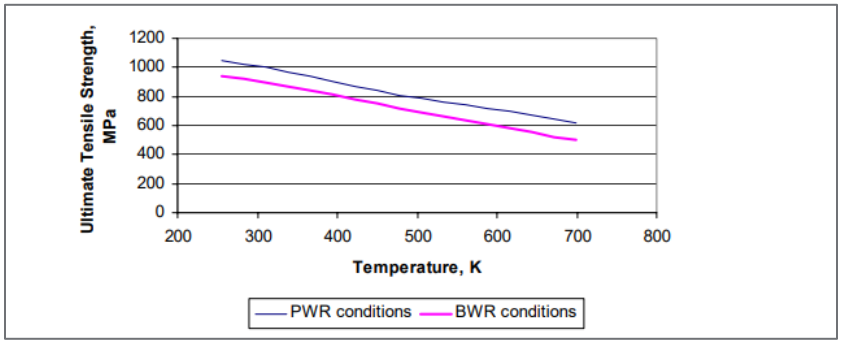

Figure A.1. Model Predictions of Ultimate Tensile Strength for PWR and BWR Conditions as a Function of Temperature for Strain of 1 x 10-4 in/in/s with Other Conditions Given in Table A.1 (Geelhood et al. 2008)

Richter et al. (1967) performed work to determine the effect of neutron irradiation on the corrosion properties of the alloys Zr3%Nb1%Sn and Zircaloy-2. Tensile and impact specimens were subjected to an integrated fast flux (E > 1 MeV) of up to 4.5×10^{19} n/cm^2 at 45°C in contact with the pool water. Analogous tests without irradiation were also performed for comparison. Tensile tests were performed at room temperature, 300°C, and 450°C. The results showed that tensile strength increased along with an increase in the level of irradiation and that tensile strength was below 200 MPa for all specimens at 450°C. Results are shown in Figure A.2.

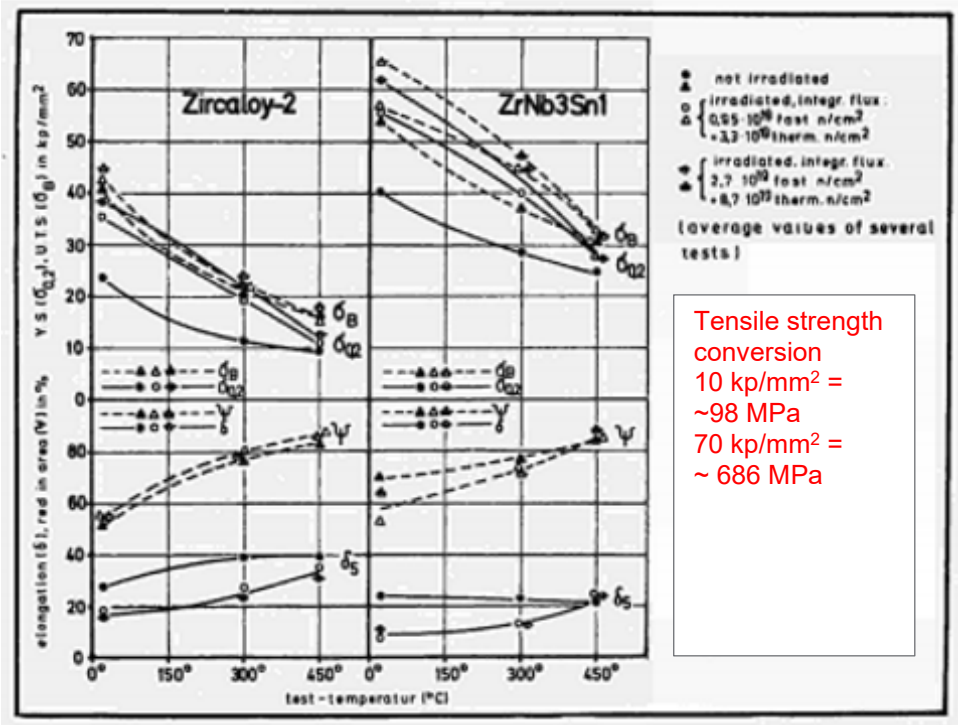

Figure A.2. Tensile and Elongation of Zircaloy-2 and ZrNb3Sn1 (Richter et al. 1967)

Zircaloy-4 PWR Cladding

Kim et al. (2005) performed ring tensile tests to obtain data regarding the uniaxial hoop direction deformation for high burnup Zircaloy-4 cladding (~57,000 MWd/tU). Several tests were performed between room temperature and 800ºC. It was determined that the ultimate tensile strength (UTS) abruptly decreases with increasing temperature beyond 400°C. Results are shown in Table A.2.

Table A.2. Mechanical Properties at Various Temperatures (Kim et al. 2005)

시편 ID	시험온도 (℃)	Strain Rate (/s)	YS (MPa)	UTS (MPa)	UE (mm/mm)	TE (mm/mm)
IRR_RT	RT	0.01	877.91	942.70	0.0148	0.0163
IRR_135	135	0.01	631.49	892.14	0.0207	0.0308
IRR_200	200	0.01	524.77	789.53	0.0197	0.1254
IRR_400	400	0.01	475.51	678.83	0.0264	0.1742
IRR_600	600	0.01	143.86	282.64	0.0887	1.0223
IRR_800	800	0.01	38.87	58.30	0.0237	0.2333

Balourdet et al. (1999) performed tensile tests with cladding of about 1.5% Sn and irradiated five cycles. Specimens used had various levels of corrosion (0 to 130 μm ZrO_2 thickness) and spanned temperatures from 20°C to 600°C. The results are shown in Figure A.3.

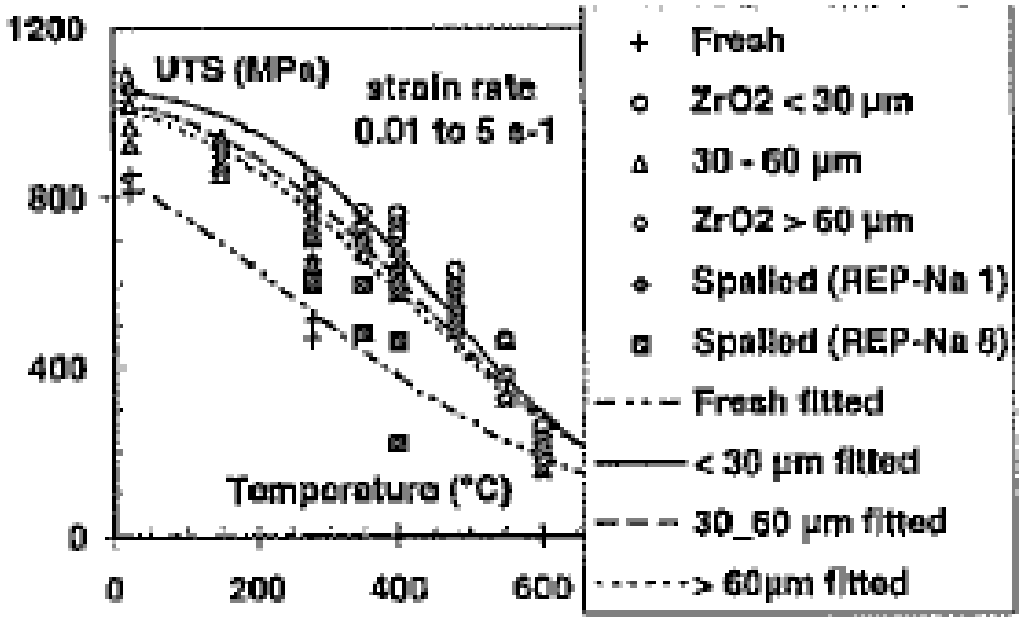

Figure A.3. Mechanical Properties at Various Temperatures (Balourdet et al. 1999)

Cazalis et al. (2005) performed hoop tensile tests for Zircaloy-4 as well as ZIRLO™, M5® (five cycles), and M5® (six cycles) ranging from 280°C to 800°C. Descriptions of the test specimens are provided in Table A.3. Results are displayed in Figure A.4.

Table A.3. Hoop Tensile Samples (Cazalis et al. 2005)

Fuel rod cladding type	Fuel rod	Reactor	Rodlet burnup (GWd/tU)	Oxide (μm)
ZIRLO™	A12	Vandellos 2	~75	80-100
5 cycle M5™	Q12/4012	Gravelines 5	58	15-20
6 cycle M5™	N05/4021	Gravelines 5	~75	15-20
5 cycle Zy-4	1055,M05,1070 P07	Gravelines 3+2 Gravelines 5	57-64	15 - 130

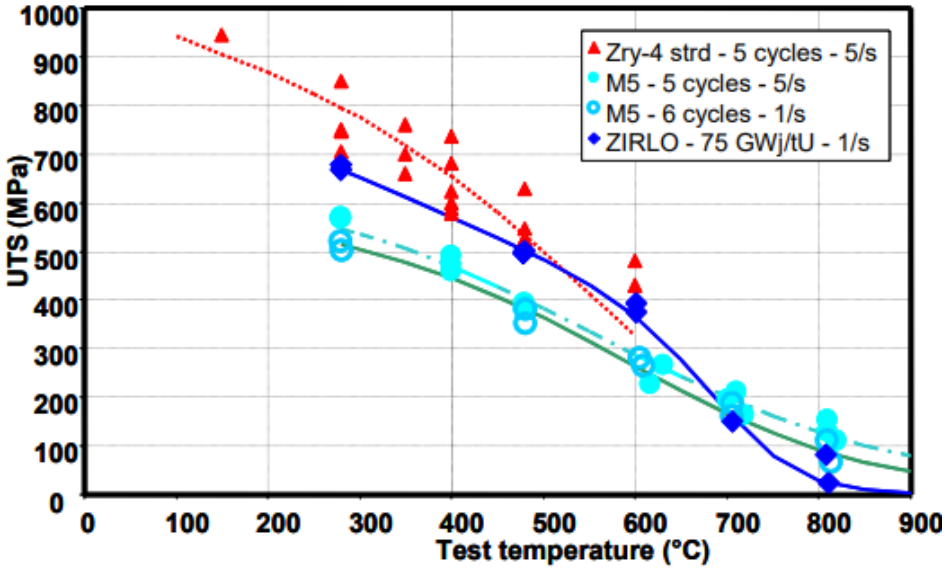

Figure A.4. Ultimate Tensile Stress as a Function of Temperature (Cazalis et al. 2005)

Geelhood et al. (2008) modeled predicted yield stress for PWR (Zircaloy-4) and BWR (Zircaloy -2) conditions as a function of temperature, fast neutron fluence, cold work and strain rate. Table A.1 above shows the parameters of the model. Figure A.1 shows the results of the model. The predicted values at 700K (427°C) are ~600 MPa with a standard deviation of +-67 MPa.

ZIRLO™ PWR Cladding

Cazalis et al. (2005) performed hoop tensile tests for Zircaloy-4 as well as ZIRLO™, M5® (five cycles), and M5® (six cycles) ranging from 280°C to 800°C. Descriptions of the test specimens are provided in Table A.3. Results from the tests are displayed in Figure A.4.

Hoon et al. (2020) examined the effects of hydrogen precipitation on the mechanical properties of Zircaloy-4 and ZIRLO™ alloys with uniaxial tensile tests at room temperature and at 400°C. Data from these tests are displayed below in Figure A.5 and Figure A.6.

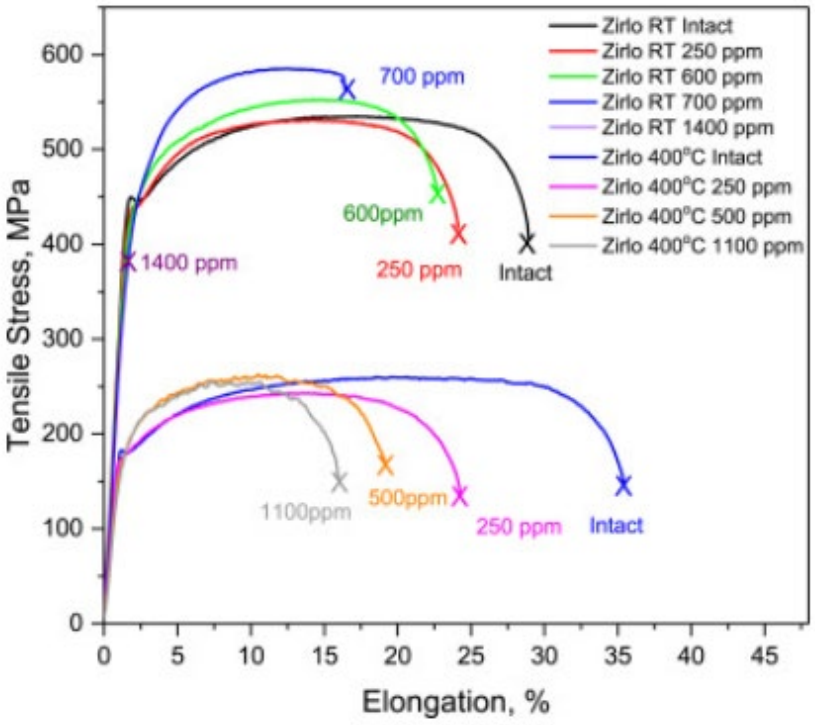

Figure A.5. Tensile Stress as a Function of Elongation Percent (Hoon et al. 2020)

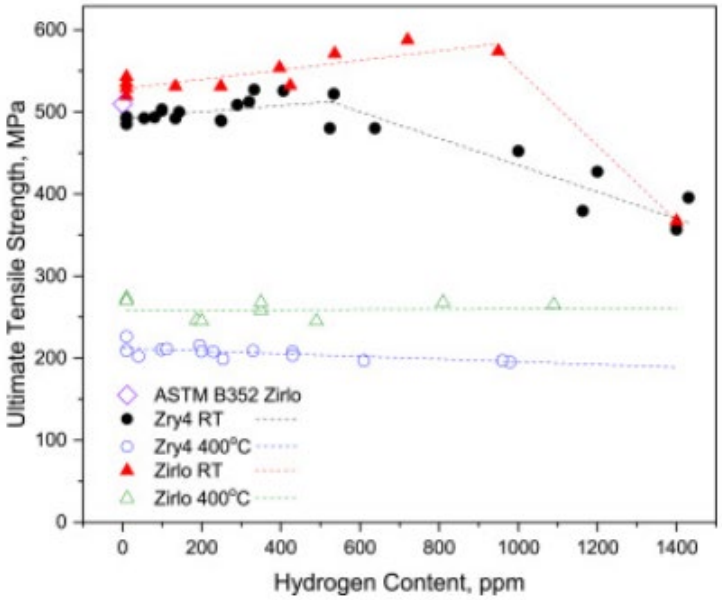

Figure A.6. Ultimate Tensile Strength as a Function of Hydrogen Content (Hoon et al. 2020).

M5® PWR Cladding

Cazalis et al. (2005) performed hoop tensile tests for Zircaloy-4 as well as ZIRLO™, M5® (five cycles), and M5® (six cycles) ranging from 280°C to 800°C. Descriptions of the specimens tested are provided in Table A.3. Results from the tests are displayed in Figure A.4.

The technical report *Development of M5® Cladding Material Correlations in the Transuranus Code* (Kecek et al. 2016) assembled previous research and data found in open literature on material properties of structural material. Yield stresses adapted from Stern et al. (2009) and Cazalis et al. (2005) are displayed in Figure A.7, and the yield strength as a function of strain rate for unirradiated M5®, irradiated Zircaloy-2, and irradiated and unirradiated Zircaloy-4 from Machiels (2020) are shown in Figure A.8.

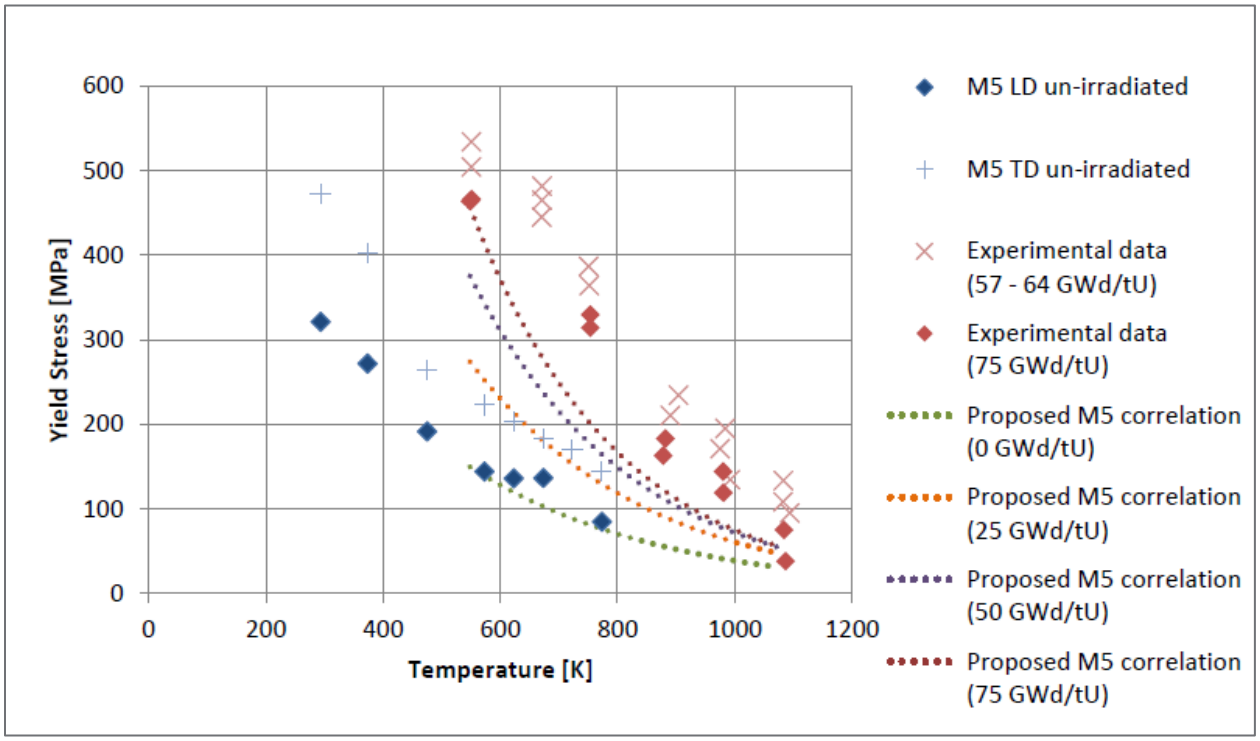

Figure A.7. Yield Stress as a Function of Temperature and Burnup. LD = longitudinal TD = transversal directions (Kecek et al. 2016).

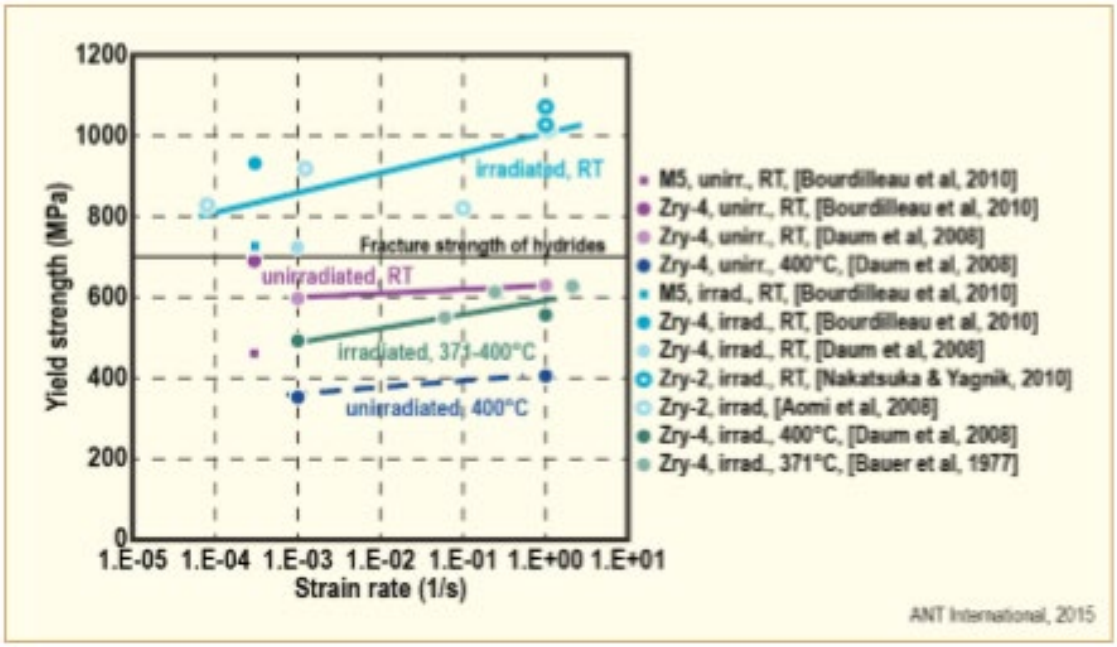

Figure A.8. Yield Strength as a Function of Strain Rate (Machiels 2020)

A.2 Fuel Assembly Hardware

The literature for fuel assembly hardware presented below is to account for materials found in the guide tubes, spacer grids, and lower and upper end fittings. The materials of interest are 304L stainless steel, high nickel alloys (Inconel), and zirconium-based materials used in the construction of fuel assemblies. Zirconium-based materials are not covered here, assuming the properties of these materials would be encompassed by the fuel cladding literature review found in the previous sections.

304L Stainless steel

Raghuram et al. (2016) investigated two grades of austenitic stainless-steel: ASS 304L and ASS 316L. Tensile tests were conducted at three different strain rates (0.0001, 0.001, and 0.01 s^{-1}) and at temperatures ranging from 50°C to 650°C. Ultimate tensile strength is shown below in Figure A.9. Note that these data do not include irradiated 304L stainless steel.

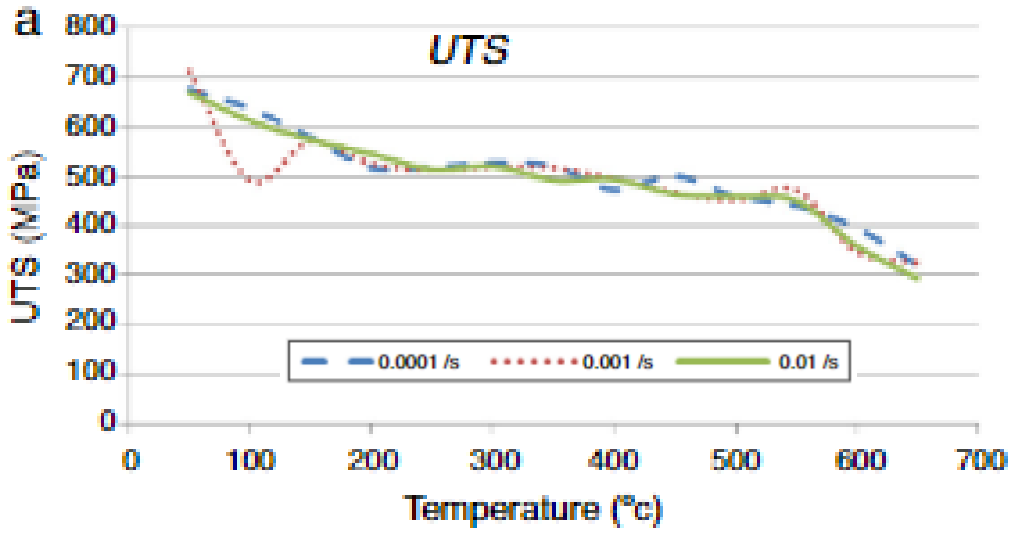

Figure A.9. Ultimate Tensile Strength as a Function of Temperature for Three Different Strain Rates (Raghuram et al. 2016)

Armijo et al.(1965) documented experimental properties of Type-304 stainless steel as a function of cold work, neutron radiation, and temperature. Table A.4 summarizes the engineering properties of irradiated and nonirradiated 304 stainless steel at room temperature.

Table A.4. Summary of Engineering Properties of 301 and 304 Stainless Steels (Armijo et al.1965). *Value of 150 * 10^3 lb/in^2 is ~ 1034 MPa and 75 * 10^3 lb/in^2 is ~517 MPa.*

Summary of Engineering Properties of 18%Cr-8%Ni Austenitic Stainless Steels

Materials AISI Designation	Testing Temperature		0.2% Yield Strength		Tensile Strength		Total Elongation,	Remarks & Reference
	(°F)	(°C)	10^3lb/in.^{2}	10^3kg/cm^2	10^3lb/in.^{2}	10^3kg/cm^2	0/0	
	85	(30)	110	7.7	150	10.5	11	
301 (half-hard)	800	(430)	96	6.7	110	7.73	4	
	1200	(650)	65	4.6	75	5.3	5	Sheet Specimens, strain rate 0.0005 in./(in. s) (Ref. 3)
	85	(30)	145	10.2	175	12.3	12	
301 (full-hard)	800	(430)	115	8.1	130	9.1	3	
	1200	(650)	70	4.9	80	5.6	4	
304 (annealed) Nonirradiated	Room Temperature		37.5	2.6	90.0	6.3	50.2	Radiation exposure 5.4 x 10^{19}n/cm^2 [a], no temperature given (Ref. 7)
Irradiated			82.0	5.75	104.8	7.35	–	
304 (annealed) Nonirradiated	Room Temperature		72.2	5.1	107.5	7.5	46	Radiation exposure 2.04 x 10^{19} n/cm^2 at 120°F (50°C) (Ref. 6)
Irradiated			126.0	8.85	126.9	8.9	32	
304 (annealed) Nonirradiated	Room Temperature		77.2	5.43	107.5	7.55	46	Radiation exposure 1.3 x 10^{20}n/cm^2 at 120°F (50°C) (Ref. 6)
Irradiated			129.3	9.1	126.9	8.9	31	
304 (annealed) Nonirradiated	Room Temperature		77.2	5.4	107.5	7.55	46	Radiation exposure 3.87 x 10^{21} n/cm^2 at 120°F (50°C) (Ref. 6)
Irradiated			129.2	9.1	129.4	9.1	50	

[a] Unless otherwise noted, integrated neutron exposures refer to neutrons whose energies are greater than 1 MeV.

Inconel Alloys

The Westinghouse report *Neutron Irradiation Effects on the Tensile Properties of Inconel 718, Waspaloy, and A.286* (Westinghouse Astronuclear Laboratory 1971) details experiments performed to obtain statistical data for the design and comparative radiation effects information for Inconel 718, Waspaloy, and A.286. Sheet tensile specimens of the three structural alloys were irradiated at 585°R in the Plumb Brook Reactor and then tested at temperatures from 540°R (26.85°C) to 1940°R (804.63°C). Inconel 718 data are displayed in Figure A.10 and Table A.5.

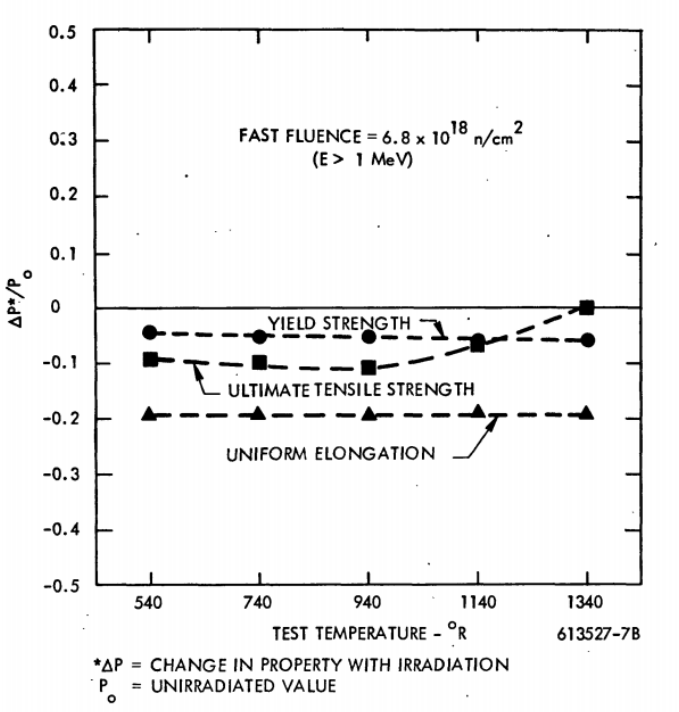

Figure A.10. Tensile Properties of irradiated Inconel 718 (Westinghouse 1971)

Table A.5. Inconel 718 Tube Test Results (Westinghouse 1971). **105 ksi ~ 724 MPa and 192 ksi ~ 1324 MPa*

INCONEL 718 TUBE TEST RESULTS

Specimen Number	Test Temp. (°R)	Thermal Fluence (E <0.48 eV) (n/cm^2)	Fast Fluence (E > 1 MeV) (n/cm^2)	0.2% Offset Yield Strength (ksi)	Ultimate Strength (ksi)	Uniform Elongation (%)	Total Elongation (%)
10	1140	0	0	158.6	192.1	11.1	11.8
4	1140	2.2 (18)	3.4 (16)	153.6	187.1	11.2	11.2
3	1240	8.0 (18)	5.4 (16)	150.7	185.0	7.6	12.9
11	1340	0	0	156.4	190.7	9.5	10.8
8	1340	7.0 (18)	7.1 (16)	154.3	195.7	5.7	10.4
5	1440	1.0 (19)	9.2 (16)	145.7	185.7	8.2	12.9
12	1540	0	0	140.7	173.6	5.6	10.6
1	1540	2.2 (18)	3.0 (16)	140.7	167.1	4.4	6.7
2	1640	7.6 (17)	1.8 (16)	122.9	130.0	5.7	9.2
9	1740	0	0	107.1	110.0	5.1	8.0
6	1740	4.7 (18)	5.0 (16)	96.4	105.0	3.1	6.1

A.3 References

Armijo JS, JR Low, and UE Wolff. 1965. "Radiation Effects on the Mechanical Properties and Microstructure of Type-304 Stainless Steel." *Nuclear Applications* 1(5):462-477, doi:10.13182/NT65-A20558

Balourdet M et al. 1999. "The PROMETRA Programme: assessment of mechanical properties of zircaloy-4 cladding during an RIA." SMIRT15 – 15th International Conference on Structural Mechanics in Reactor Technology, Vol. II, p. 485, Seoul, Korea.

Beyer CE and KJ Geelhood. 2013. *Pellet-Cladding Mechanical Interaction Failure Threshold for Reactivity Initiated Accidents for Pressurized Water Reactors and Boiling Water Reactors*. PNNL-22549, Pacific Northwest National Laboratory, Richland, WA.

Cazalis B et al. 2005. "The Prometra Program: A Reliable Material Database for Highly Irradiated Zircaloy-4, ZIRLO™ and M5® Fuel Claddings." 18th International Conference on Structural Mechanics in Reactor Technology (SMiRT 18), Beijing, China, ASTM.

Geelhood KJ, CE Beyer, and WG Luscher. 2008. *PNNL Stress/Strain Correlation for Zircaloy*. PNNL-17700, Pacific Northwest National Laboratory, Richland, WA.

Hoon L, K-m Kim, J-S Kim, and Y-S Kim. 2020. "Effects of hydride precipitation on the mechanical property of cold worked zirconium alloys in fully recrystallized condition." *Nuclear Engineering and Technology* 52(2):352-359, ISSN 1738-5733.

Kecek A, K Tuček, S Holmström, and P van Uffelen. 2016. *Development of M5® Cladding Material Correlations in the TRANSURANUS Code: Revision 1*, EUR 28366 EN, Publications

Office of the European Union, Luxembourg, 2016, ISBN 978-92-79-64655-3, doi:10.2789/332093, JRC100644.

Kim S, J Bang, and D Kim. 2005. “Evaluation of mechanical strength and ductility of high burn-up nuclear fuel cladding.” *Proceedings of the 2005 Water Reactor Fuel Performance Meeting*, Atomic Energy Society of Japan, p. 1236.

Machiels A. 2020. *Effect of Hydride Reorientation in Spent Fuel Cladding—Status from Twenty Years of Research*. EPRI Technical Report 3002016033, J Kessler and Associates, LLC, Charlotte, NC.

Richter HW, W Ruckdeschel, E Spalthoff, and E Starke. 1967. *Influence of Neutron Irradiation on the Mechanical Properties and the Corrosion Behaviour of ZrNb3Sn1 and Zircaloy-2.* EURAEC Report No. 1795, European Atomic Community, Brussels, Belgium.

Raghuram KD, HN Krishnamurthy, A Balu, AK Gupta, and SK Singh. 2016. “Mechanical properties of Austenitic Stainless Steel 304L and 316L at elevated temperatures.” *Journal of Materials Research and Technology* 5(1):13-20, ISSN 2238-7854.

Stern A et al. 2009. “Investigations of the Microstructure and Mechanical Properties of Prior-β Structure as a Function of the Oxygen Content in Two Zirconium Alloys.” In *Proceedings of 15th International Symposium on Zirconium in the Nuclear Industry*, Sunriver, OR, ASTM.

Westinghouse Astronuclear Laboratory. 1971. *Neutron Irradiation Effects on the Tensile Properties of Inconel 718, WASPALOY, and A-286*. OSTI.gov, www.osti.gov/servlets/purl/4244226.

Pacific Northwest National Laboratory

902 Battelle Boulevard
P.O. Box 999
Richland, WA 99354
1-888-375-PNNL (7665)

www.pnnl.gov* | *www.nrc.gov